Geomorphic Features of Quaternary Glaciation in the Middle Section of the Tayantaweng Range, on the southeastern Qinghai-Tibet Plateau

Abstract: We present geomorphological evidence for multiple glacial fluctuations during the Quaternary in the middle section of the Tayantaweng Shan, which is situated at the transition zone of the southeastern Qinghai-Tibet Plateau and the Yunnan-Guizhou Plateau. To reconstruct the history of glacial evolution during the Quaternary Glaciation, we present a ~13000 km^2 geomorphologic map (1:440,000) for the Quaternary glaciations, as well as three electron spin resonance (ESR) ages and three optically stimulated luminescence (OSL) ages from the landforms. By integrating these with ages from previous studies, five major glacial advances are identified during marine oxygen isotope stages (MIS) 6, 3, 2, late glacial and 1. This glacial chronology is in reasonable agreement with existing glacial chronologies from other parts of the Hengduan Mountains and surrounding mountains. Glaciers had extended to the Yuqu River during the glacial maximum advance (MIS 6), but. became successively more restricted from MIS 3 to MIS 1. The glacial patterns show that precipitation brought by the south Asian monsoon might play a primary role in driving glacial advances during the last glacial period in the southeastern Qinghai-Tibet Plateau.

Keywords Qinghai-Tibet Plateau; Tayantaweng; glacial landform; ESR dating; OSL dating

Introduction

With its marginal mountain ranges, the Qinghai Tibet Plateau (QTP) has the most abundant glacial action at the highest altitude, with the exception of the two polar regions (Shi et al. 1988). Therefore, it has a far-reaching influence on the patterns of global and regional atmospheric circulation, and plays an important role in research regarding the dynamic mechanisms which drive global environmental changes (Benn and Owen 1998; Dortch et al. 2013; Li, 1991; Shi 2002). Reconstructing the extent, timing, nature, and geologic impact of glaciation on the QTP is important because of the central role of glaciation in paleoclimate reconstructions and geological evolution models, and provides important content for the geomorphic evolution of the mountain system (Cui et al. 2011; Liu et al. 2011; Norto et al. 2010). From the Quaternary Period, the results of large amounts of glacial erosion and accumulation clearly remain on the QTP. These have become important environmental indexes for the regional environmental evolution pattern, as well as for predictions of future climate change trends (Li et al. 1986; Owen and Dortch 2014; Owen et al. 2009; Tschudi et al. 2003; Zhang et al. 2016b). A number of plateau-wide glacial reconstructions exist for the QTP (Li 1991; Lehmkuhl and Owen 2005), and in recent years the application of ArcGIS and remote sensing technologies, combined with traditional field geomorphologic survey methods, has made the reconstruction of glacial landforms more accurate (Lindholm and Heyman 2015; Fu et al. 2012), and promoted further research on the development of Quaternary glacial landforms on the QTP. However, the extent and timing of glaciation in the QTP remain poorly documented. In order to continue to develop documented evidence for former glaciations, we present detailed glacial geomorphological features and dates of deposits in the middle section of the Tayantaweng Shan on the southeastern QTP.

Situated to the west of the Hengduan Mountains, the middle section of the Tayantaweng Shan is at the transition zone of the southeastern QTP and the Yunnan-Guizhou Plateau (Figure 1). During the Quaternary period, numerous glacial actions occurred on the large areas of planation surface in the region. Glacial erosion could also be mapped using the accumulation landforms, particularly the well-preserved glacial deposits. Maritime in nature and sustained by precipitation from the South Asian monsoon, the advance and retreat of the Quaternary glaciers in this region thus directly reflect fluctuations in the South Asian monsoon. This special geographical location gives particular importance to Quaternary glacial research in the middle section of the Tayantaweng Shan.

We have investigated the glacial landforms of the middle section of the Tayantaweng Shan from 2014 to 2017. Several ESR dating results are presented in Zhang and Chai (2016a), which suggest at least four major glacial events during MIS 6, 3b, 2, and 1. However, there is still an essential lack of a detailed survey of glacial geomorphology and numerical dating of glacial sediments. In order to obtain additional geomorphic features and numerical dating evidence, this study focuses on detailed geomorphology as well as OSL and ESR dating of glacial landforms in the middle section of the Tayantaweng Shan. This work forms a basis for understanding the characteristics of past glaciations in this area. Furthermore, it also allows for a more comprehensive comparison of the timing and extent of Quaternary glaciations between the Hengduan Mountains and other glaciated areas in the southeastern QTP.

1 Regional Geographic-geological Background

The middle section of the Tayantaweng Shan (30°45′N–30°11′N, 96°30′E–97°30′E) is located between the Nujiang River and Lantsang River in the western region of the Hengduan Mountains (Figure 1). (Downstream, the Nu Jiang is known as the Salween River.) The mountains extend in a NW-to-SE direction, with altitudes of approximately 4200 m. The terrain is higher in the north and west, and lower in the south and east. Two levels of planation surface have developed, with the highest level reaching up to between 5100 and 5200 m (Yang et al. 1983). On the Yuqu River, flowing in a NW-to-SE direction, the upstream altitude is above 4300 m and the main valley is a typical wide valley with wide and shallow riverbeds and a developed flood plain. Its width is between 1 and 2 km, and it is the largest valley in the Changdu Region (Shi et al. 1988). The lithology is mainly composed of granite, limestone, phyllite, sandstone, and slate.

This area is mainly influenced by the south Asian monsoon, with an annual precipitation of 474.2 mm (Changdu meteorological station at 3307 m), and an annual average temperature of 7.6 ℃ (Su and Pu 1996). Contemporary glaciers are mainly distributed on both sides of the Yuqu River, consisting of approximately 100 small glaciers, with an area of 28.32 km^2. The mean equilibrium line altitude (ELA) in the study area for the contemporary glaciers is approximately 5400 m according to Su and Pu (1996). The glacier shape types include cirque glaciers and hanging glaciers (Su and Pu 1996). In accordance with the development conditions and physical nature of the glaciers, the research area has been determined to have the characteristics of maritime glaciation (Shi and Liu 2000).

2 Geomorphologic Features

2.1 Characteristics of the glacial erosive landforms

The most common glaciated landforms were "U" shaped valleys (Figure 2A), with lengths between 4.5 and 26 km, widths between 4 and 5 km, and depths between 200 and 500 m. In the glacial valley at one side of the Nujiang River (Figure 2B a–c), glacial action was evident upstream, whereas the downstream section showed a "V" shape due to fluvial incision. The valley on the bank of the Yuqu River mainly displayed a gentle "U" shape (Figure 2B d–f). Additionally, the longitudinal section showed that the glacial valley on the bank of the Nujiang River was steep, whereas the valley on the bank of the Yuqu River was gentle (Figure 2B g). In addition, owing to the differences in glacial erosion between the main and branch valleys, a large number of hanging glacial valleys formed on both sides of the main valley in the research area (Figure 3d). These combined with the main valley to form composite-type valley glaciers of different scales, such as the typical ones of the Quzha River (Figure 3e), Juequ River (Figure 3f), and Ruqu River. A total of 191 glacial valley polygons in the research area were digitized, with a total area of 2100 km^2, which accounted for 12% of the total area of the research region.

Furthermore, there are a large number of cirques in the research region. The majority of these cirques are empty, whereas only a small number of the inside or headwall cirques retain small cirque glaciers or hanging glaciers (Figure 3a, 3b). The altitudes of the cirque bottoms were within the range of 4800 to 5400 m. Meanwhile, typical roche moutonnées (Figure 3b, 3c), comb-shaped arêtes, and pyramid-shaped horns were preserved in the research region (Figure 3f).

2.2 Geomorphic features of the glacial deposits

Marginal moraines are ridge-shaped constructional landforms created along the margins of glaciers, including arc-shaped moraines and lateral moraines formed by valley or cirque glaciers. Moraines formed by valley glaciers occur along valley sides. A total of 159.43 km^2 marginal moraine polygons were mapped. The morphostratigraphic relationships between landforms of different glacial stages were examined together with the surface weathering characteristics, altitude, and extent of the moraines in the Quzha Valley, Juequ Valley, and Ruqu Valley (Figure 4).

2.2.1 Quzha and Qinggulong Valleys

Four groups of moraines developed in the Quzha Valley ((Figure 4A). The moraine (QM4) at the valley's mouth was located 30 km from the valley source, with an altitude of 4356 m, and height of 2.4 m. It covered bedrock, with a valley mouth lithology composed of slate. Its terminal reached the main valley of the Yuqu, and upstream it extended to a place near a moraine-dammed lake. On profile SECTION Z 1 of the 214-highway (Figure 5A), which was located north of the valley mouth, a small amount of granite gravel with boulder diameters between 50 and 100 cm is preserved on the crest of the moraine. Additionally, soil had developed on the surface of the deposits. The components of the lower gravel layer included granite, metamorphic rock, and limestone. The granite gravel displayed good roundness, and was observed to be severely weathered. The minerals had intense alteration, and easily incurred exfoliation. The middle of the section was a coarse sand layer supported by gravel, and contained a small number of suspended cobbles with diameters of 20 cm. This layer also had an abrupt contact with the underlying bed. The upper part was a mixed deposit layer consisting of granite and slate clasts, with a gravel content > 95%. The granite gravel was observed to be severely weathered, and the surface of the cobbles could be broken by grasping it in the hand.

The profile SECTION Z2 (Figure 5A) was located on the lateral moraine near the lake, with an altitude between 4400 and 4500 m, which is approximately 35 m higher than the contemporary riverbed. The roadside exposure profile showed that the lithology of the lateral moraine mainly included limestone and granite, with the upper section a mixed deposit layer of a gravel structure, and the lower part made up of a developed ice–water interlayer. Additionally, the thickness of the sand layer exceeded 50 cm. The granite gravel on the crest of the lateral moraine was observed to be severely weathered. In accordance with the location of the deposits at the upstream lateral moraine, as well as at the valley mouth of the lake in the Quzha Valley, it was determined that glacier melting during the interglacial period had a long-term transformation effect on the terminal moraine deposited at the valley mouth. With respect to the moraine preserved on the upper bedrock at the valley mouth opposite the Quzha Valley, it was found to have a gravel structure and weathering features similar to M4. Therefore, these two trough valleys may have converged into the Yuqu River during the maximum glaciation period.

The terminus of moraine QM3 was located 15 km from the source, and was between approximately 10 and 15 m higher than the contemporary riverbed (Figure 5A). It had intermittently developed on the northern side of the base of the trough valley, and the crest was covered by herbaceous vegetation. Parts of these areas were covered by talus and a proluvial fan, owing to the serious destruction effects of the hanging valley, as well as the deposits on both sides.

The moraine at the intersection location (4810 m) of the upstream trough valley in the Quzha River was found to be preserved in the forms of a moraine platform and a terminal moraine (QM2, Figure 3f). The moraine platform had been split into eastern and western sections by water flow during a later phase: it has a length of 700 m, width of 200 m, height of 7 to 8 m, and distance of approximately 8 km from the upstream cirque. The flat crest was found to be covered by weakly weathered granite gravel of various sizes. At an altitude of 4775 m, below the moraine platform, there was one terminal moraine crossing through the front end of the valley mouth. Its main part consisted of loose bodies containing gravelly sand, and its crest was covered by a large amount of differently shaped gravel in a scattered pattern.

Two to three rows of new terminal and lateral moraines, without a developed soil layer, were distributed between 1 and 3 km from the lower end (at 5200 m) of the contemporary glacier at the source of the Quzha Valley. Their lithology was monzonitic granite, with mainly angular gravel. Additionally, glacial boulders with maximum sizes of 3 × 2.5 × 1.7 m were found to be scattered on the crest in this section.

In addition, Qinggulong Village (4370 m), which is located on the south side of the Quzha Valley, was found to have many groups of preserved moraine in clear and complete formations (QM4, Figure 5B) The moraine at an altitude of approximately 4300 m on the northeastern side of the entrance to Qinggulong Village was approximately 12 km from the source of the former glacier. It had a length of approximately 50 m, and it was 20 to 25 m above the contemporary river bed. The profile SECTION Z3 (Figure 5A) showed that it consisted of a mixed deposit gravel structure. Additionally, there was cementation observed among the gravel. Its lithology was dominated by granite, phyllite, and slate, and the gravel showed rounding, which was possibly due to experiencing a water flow transformation effect during a later phase. This indicated that the glaciers at that time may have extended from the glacier accumulation area (peak 5600 m) of the ancient planation surface on the western side of Qinggulong Village, towards the upstream bank of the Yuqu, which then produced deposits in the valley mouth.

Moraine QM3 was observed to be distributed within an altitude range of 4600 to 5250 m, and extended from upstream to downstream for approximately 7 km. The most obvious moraines were the lateral and downstream terminal moraines, which displayed a parallel symmetric distribution (Figure 6). The lateral moraine dam was observed to be a mound shape, and had a relative height of approximately 20 m, with an obvious ridge feature on the crest. Additionally, granite boulders with diameters of 300 × 150 × 100 cm were scattered on the surface, and the profile of exposed and mixed deposit showed that its lithological composition mainly consisted of granite and phyllite, which displayed a low degree of weathering. Moreover, the arc-shaped terminal moraine, which had a large relief and connected with the lower limb of this set of lateral moraine, had an altitude range between 4600 and 4860 m. The terminal moraine's width was between 250 and 300 m, which indicated that glaciation had a slow recession rate in this location. At the same time, the surface of the terminal moraine was covered by a large number of granite boulders.

The upstream QM2 moraine in Qinggulong Village was distributed in the valley bottom in the form of a lower lateral and terminal moraine (Figure 6). The lower lateral moraine extended downwards over 4.5 km, with heights between 2 and 6 m. Additionally, it was preserved in the form of a terminal moraine at an altitude of 5000 m at the end position. It was observed that granite gravel with obvious edges rested on the crest, and the weathered halos had a width ranging between 0.5 and 1 mm.

The terminal moraine QM1 was preserved at altitudes between 5175 and 5320 m in the cirque, extended downwards to 5250 m at the exit of the cirque (Figure 3b), which was 60 to 75 m above the valley bottom. This deposit displayed a greyish-yellow colour and an arcuate distribution, and lay across the cirque mouth. It was observed to be steep outside and gentle inside, and extended downwards for approximately 0.75 to 1.5 km, until it reached the upper part of the rock step of the cirque mouth. It was observed that monzonitic granite gravel with a large volume and obvious edges was usually distributed on the crest of the moraine ridge. From the point of view of the exposed profile of the moraine ridge, the lithology of the moraine consisted of granite, and it was characterized by a fresh gravel surface and an extremely low degree of weathering.

2.2.2 Juequ Valley

The high lateral moraine in the Juequ River extended from the Qinqia Village (4550 m) to the banks of the Yuqu River (Figure 4B), and was preserved in the form of a terminal moraine (JM4) (Figure 7B). The terminal moraine at the valley mouth had an altitude ranging between 4350 and 4500 m, 85 to 140 m above the riverbed. A large number of granite boulders were observed to be scattered on the crest of the ridge, with a maximum particle size of 450 × 200 × 150 cm. The amount of granite gravel gradually decreased downwards to the Yuqu river bed, and the surfaces of some of the boulders were observed to be severely weathered. A yellow-grey weathering halo measuring between 1.5 and 2 cm thick was observed, and weathered debris was scattered around the boulders (Figure 3h). The SECTION J4 profile (Figure 7A) of the exposed deposits was approximately 25 km from the source of the trough valley. The deposits were mainly coarse sand, and also contained granite, sandstone, and limestone gravel, with a good suspension grounding in the middle. A portion of the granite gravel was observed to be intensely weathered. The crest of the lateral moraine near the Qinqia Village was found to be 120 to 150 m higher than the valley base. The exposed sediment profile SECTION J3 (Figure 7A) near the highway was located approximately 10 to 15 km from the valley head. A large amount of granite gravel was distributed on the crest, with a maximum particle size of 250 × 250 × 100 cm. The deposit profile could be divided into four layers, where the gravel layers alternated with the coarse sand layers. The gravel layers had a high degree of roundness, and their lithology was determined to be granite and sandstone. The gravel was observed to have a high degree of weathering, and the granite gravel with particle sizes of 1.5 cm became loose when touched by hand. The coarse sand layer did not contain mud, and had a development of sand ripple bedding. Additionally, a good degree of roundness was observed in the pebbles.

Moraine JM3 in the Juequ Valley was preserved at the intersection location between the main valley and the branch valley in the form of a terminal moraine (Figure 3g), with a crest altitude ranging between 4600 to 4770 m. The crest was approximately 40 m above the riverbed of the Juequ River, and displayed an arc shape, convex towards the downstream area. It was located 13 km from the trough valley, with a width of 640 m and a length of 4 km. A large amount of granite gravel was scattered on the crest, and low shrubs were observed to be growing. The terminal moraine was found to be mainly a combination of till and glacifluvial deposits. The glacifluvial deposits were widely distributed in this area, and were observed to be located at the outer margin of the terminal moraine, as well as close to the riverbed. The deposit profile of SECTION J1 (Figure 7A) mainly consisted of grey and light-yellow fine silt, up to 2.8 m thick and with no bedding. It contained granite and sandstone moraine gravel with good roundness, and diameters between 5 and 10 cm. The moraine was developed at a relatively higher position, and its deposit profile was SECTION J2 (Figure 7A). The main lithology contained granite, sandstone, and limestone. Additionally, light-grey clay was found to be preserved in the lower part of the moraine.

Moraine JM2 in the Juequ River extended to approximately 3 km from the cirque mouth, and its terminal altitude was determined to be 4850 m. The lateral moraine on both sides formed a moraine lake (Cuo Ga Xiong) through an enclosure at the terminal location, and a large amount of gravel was observed to be scattered on the moraine ridge. The proluvial fan at the exit of the hanging valley on both sides of the trough valley displayed a large destruction area in the formation of this set of moraine ridges, which had previously led to confused judgments regarding the sources of the crest gravel and deposits, and had also influenced the collection of the chronological samples.

Moraine JM1 in the Juequ River was preserved in the form of terminal moraine at a location which ranged from the contemporary glacier terminus to the rock step at the cirque mouth. The terminal altitude was 4900 m. Its clast lithology was monzonitic granite, with the glacial lake Cuo Ga located at the bottom of the cirque.

2.2.3 Ruqu River

It was found in this study that moraines in the Ruqu River basin were distributed at altitudes ranging from 4650 to 5200 m (Figure 4C, Figure 8B). Moraine RM4 was preserved as large, high lateral and terminal moraines. The high and large lateral moraine intermittently extended from the altitude of 5000 m on both sides of the trough valley, to the altitude of 4670 m at the valley mouth, with a length of approximately 10 km, and was observed to be approximately 120 to 130 m above the valley bottom. A large amount of granite gravel (boulders) was preserved on the ridge crest, with a maximum size of 300 × 128 × 130 cm. Abraded rocks were preserved at altitudes between 4790 and 4820 m upstream of the lateral moraine (Figure 3b), with granite (Figure 3d) and phyllite lithologies. The abraded granite displayed clearly preserved scratches on the top, whereas the abraded phyllite was observed to be severely weathered and broken. The terminal moraine at the valley mouth was located 25 km from the source of the trough valley, and was lying on bedrock. Its end (4630 m) extended towards the valley of the Yuqu River. The north side of the valley mouth had the largest scale, with a crest altitude of 4800 km. It was located 180 m above the Ruqu riverbed, and distributed with a large amount of scattered granite and slate gravel. In accordance with the deposit profile SECTION R1 (Figure 8A), which was exposed at the side of the highway area, the upper and lower sections were determined to be deposits of mixed gravel layers. The lower section had an angular unconformity contact with the bedrock (limestone), whereas the upper gravel layer often showed scratched limestone polygonal clasts. The middle layer was a greyish-yellow coarse sand layer interbedded with pebbles, with particle sizes between 2 and 3cm. Additionally, a thicker soil layer was developed on the crest of the deposit profile SECTION R2 (Figure 8A), on which granite gravel was observed to be scattered. The lower section was a coarse sand layer interbedded with pebbles of diameter 3 to 5 cm, and the upper section contained a mixed deposit layer.

The RM3 moraine in the Ruqu River was preserved in the form of gentle lateral moraine, with a terminal moraine at the valley bottom. These two moraine dams were observed to be completely limited in the extent of the high lateral moraine formed by the 4th group of moraine. The moraine which had been transformed by water flow was located between these two moraine dams and the terminal moraine at the valley mouth. The terminal moraine had an altitude of 4760 m, and was located at the intersection between the main valley and the branch valley, with an undulating terrain. It was located 11km from the source of the trough valley and river, at heights from 8 to 15 m. A large amount of granite gravel was scattered on the ridge crest, and the maximum particle size was determined to be 250 × 200 × 100 cm. The exposure surfaces of the deposits contained new gravel, whereas the bottom displayed a calcareous semi-cementation state.

Moraine RM2 in the Ruqu River extended to approximately 5 km from the cirque mouth, and the terminal moraine blocks of the riverbed formed a barrier lake. A large amount of granite gravel was observed to be scattered on the moraine ridge. Additionally, a thin layer of soil had developed on the moraine ridge, and sparse grassland vegetation was found to be growing in the moraine ridge area.

The newest set of moraines (RM1) was preserved within the scope of 2 km from the source of the trough valley, which could be divided into two parts, as follows: The first part was the terminal moraine end (5050 m) which was preserved in the cirque, and the second part was the downward moraine ridge end (5000 m) at the cirque mouth. It was determined that their clast lithology was granite.

According to a comparative study on the topographic conditions, glacial scale, altitude range, moraine structure and weathering degree of the Quaternary glacial landform in the study area, we can conclude that the onset of the glaciation occurred at the same time in

Jueq valley, Quzha valley, and Ruqu valley. Additionally, owing to the steep terrain, the Qinggulong valley only preserved glacial remnants from the last glacial period.

3. Methods

3.1 Field investigation and geomorphologic mapping

The field work focused on the shape, depositional features, and distribution position of the glacial landforms. The landforms and strata were divided according to their relative geomorphologic positions, forms, vegetation cover, weathering characteristics, and the mutual relationships of the moraine. To reconstruct the moraine morphostratigraphy, features such as crest morphology (sharp to round crested) and elevation points measured from GPS were used. The entire erosional and depositional landforms of the valley have been marked all along the valley and plotted on the map. We have mapped glacial landforms using the SRTM DEM with 30 m horizontal resolution, and Google Earth. The mapping was primarily performed using the ArcGIS 10.0 software package. We present a glacial geomorphological map covering 13,000 km^2, presented at a scale of 1:440,000.

3.2 OSL dating

Three OSL samples were collected from the glacial sediments at the Qinggulong Village moraine ridge (Figure 4A). A typical moraine matrix was sampled. Specifically, the surface 40–50 cm layer was stripped from the moraine, and a tube (25 cm long, 4 cm wide, sealed at one end) was completely hammered into the fresh surface, and then removed and immediately closed with a steel sheet. The tube was wrapped tightly with aluminium foil and tape to avoid water loss and exposure to light, and was assigned a field-collection number.

The samples were all processed and dated at the Luminescence Chronology Laboratory of South China Normal University, following the procedures in Lai (2010). The samples were first dry-sieved to eliminate the >300 μm grains. The fine particles were immersed sequentially in 10% diluted hydrochloric acid and 30% hydrogen peroxide to remove the carbonate and organic matter. The particles were dry-sifted to obtain the 38–63 μm fractions, which were then soaked in 35% fluorosilicic acid to remove feldspar. A small amount of 10% dilute hydrochloric acid was used in the last step to eliminate fluoride precipitates that came from reaction between the sample and fluorosilicic acid. The extracted quartz particles were scanned for purity by infrared stimulated luminescence (IRSL). High infrared signals indicate the presence of feldspar on the sample surface, which requires digestion by fluorosilicic acid again until the infrared signals vanish or decrease to a low level (IRSL/OSL < 10%), indicating sufficiently pure quartz. In the final step, a layer of silicone glue was evenly coated on a stainless-steel wafer of diameter 0.97 cm, and the sample was uniformly fixed within a diameter of approximately 0.67 cm.

The equivalent dose (*De*) was measured by the single aliquot regenerative-dose (SAR) (Murray and Wintle 2000). BDO-04，BDO-05, and BDO-06 of the samples prepared 31, 38, and 47 aliquots were measured De using the SAR. The equivalent dose (*De*) measurements were performed on an automated Risø TL/OSL-DA-20 reader. The irradiation was provided by a $^{90}Sr/^{90}Y$ beta source. The luminescence was stimulated at 130 ℃ for 40 s by light-emitting diodes producing 90% blue light (λ = 470 ± 20 nm). The stimulated light was picked up and recorded by a photomultiplier tube (EMI 9235QA) after passing through a 7.5-mm-thick Hoya U-340 filter. During the measurement, the regenerative doses and test doses were preheated at 260 ℃ for 10 s and 220 ℃ for 10 s, respectively. Figure 9 gives the OSL decay and growth curves. Previous studies suggest heat transfer as one of the factors for uncertainty in OSL dating. As such, a test at zero dose was added to the SAR protocol here to determine the effects of heat transfer on the equivalent dose measurement. The signal-to-noise ratios of BDO-04，BDO-05, and BDO-06 were 1.219 ± 0.060, 0.785 ± 0.027, and 1.053 ± 0.062，respectively, and the recycling ratios were 1.01 ± 0.07, 0.90 ± 0.04, and 0.94±0.06, respectively. The heat-transfer effect is expressed as the ratio between the corrected zero-dose luminescence and natural-dose luminescence, (L_0/T_0) / (L_n/T_n). Wintle and Murray proposed an upper limit of 5% for (L_0/T_0) / (L_n/T_n), and the samples in this study all display ratios <3%, indicating negligible effect of heat transfer.

The concentrations of U, Th, and K were measured by neutron activation analysis (NAA) to calculate the annual dose. The measured results of water content were found to be between 0.59% and 3.8%. The contribution of cosmic rays to the annual dose was calculated according to the altitude, geographical location, and sampling depth of the samples (Prescott 1994). The equations and parameters used in annual dose calculation are given in Aitken (1998). The OSL results are listed in Table 1.

3.3 ESR dating

In recent years, remarkable progress has been made in Quaternary glacial-chronology with the development of ESR. Yi et al. (2016) studied the mechanism of ESR signal change in quartz sand in moraine in typical glacier area; they suggest that ESR will provide accurate dating of ancient glacier tills for Quaternary glaciation research (Bi and Yi, 2016). To constrain the chronology of glaciation in the Juequ valley, three samples for ESR dating (JQE-01, JQE-02, JQE-03) were collected from natural or human-made sections from the moraines in the Juequ Valley (Figure 4B, Figure 7A). The samples were kept in opaque bags to prevent exposure to sunlight. During transportation, the samples were carefully packaged to avoid grinding, collision, and heating. The samples were pre-treated in the State Key Laboratory of earthquake dynamics, Institute of Geology, China Earthquake Administration, Beijing following the procedure described in Liu et al. (2010). The quartz Ti-Li centres were chosen as dating signals and measured with a BRUKER ER041XG X band spectrometer. The specifications of the measurement are as follows: low-temperature (liquid nitrogen, 77 K) conditions; microwave power, 5 mW; microwave frequency, 9.46 GHz; modulation frequency, 100 kHz; and modulation amplitude 0.16 mT. The Ti-Li centre intensity was measured from the top of the peak at g = 1.979 to the bottom at g =1.913 (Rink et al, 2007; Liu et al, 2013. The Ti signal intensities increased with additional increasing doses. All of the samples were measured six times in different directions to obtain the average intensity.

For all samples, the equivalent dose (*De*) values and their individual errors were determined from the dose response data fitted with a single saturating exponential (SSE) function using the protocol (and the software) described by Yokoyama et al. (1985). A least-squares analysis was used to fit the data points based on different artificial irradiation doses and corresponding signal intensities using linear fits (Figure 10). All De values were obtained assuming complete bleaching. The dose rate (*D*) was calculated from the concentrations of U, Th, and K of each sample (Aitken 1998). The concentrations of U and Th were obtained using a thick source Daybreak 530 Model alpha counter, and the K concentrations were determined by atomic absorption. Finally, the annual dose rate was estimated from these radioactive elements, along with the water content and the cosmic ray contribution, which were estimated and calculated following the formulas suggested by Prescott and Hutton (1994). The details of the sampling sites, the results of the dating, and the correlated parameters are listed in Table 2.

4 Results

The OSL and ESR results are listed in Table 1 and Table 2, respectively. We have referenced Zhao et al. (2011) for the age control points of the MIS stage. In the Qingguling Valley, from the dating result (17.3 ± 1.25 ka) of moraine BDO-4 from the lower lateral side (QM 2), we suggest the moraine formed during the late stage of the last glacial period. The dating results of moraines BDO-5 and BDO- 6 from the higher lateral side (QM 3) are 31.38 ± 3.48 ka and 25.78 ± 1.98 ka, respectively, corresponding to MIS 2. In the Juequ valley, the oldest moraine JM4 is dated to 212 ± 21.34 ka and 240.3 ± 49.8 ka with two ESR ages, suggesting a glacial advance during MIS 6. JM3 yields ESR dating of 51.78 ± 10.62 ka, corresponding to a glacial advance during MIS 3.

5 Discussion

5.1 Resetting of ESR and OSL signals in glacial environments

A study of the Quaternary glacial sediments on the QTP and the surrounding mountains shows that from the accumulation zone to the terminal, the rock debris entering the glacier, following repeated alternative stretching and compression flows and possibly passing through a shear surface inside the glacier, has a higher chance of exposure (Richards 2000). Moving at the glacier surface, the signal from fine particles at the moraine ridge top could be completely bleached, providing reliable OSL results, and supraglacial deposits are demonstrated to be more suitable for OSL dating than tills (Benn and Owen 2002; Fuchs and Owen 2008; Richards 2000). The moraine ridge at Qinggulong is well preserved, and samples BDO-5 and BDO-6 were both collected from the QM3 ridge, whereas BDO-4 was sampled from the QM2 ridge. The ages of the three samples are 31.38 ± 3.48 ka, 25.78 ± 1.98 ka, and 17.3 ± 1.25 ka, respectively. The reason for the discrepancy is that the age of BDO-5 was overestimated.

Sample BDO-4 and BDO-6 were collected at the top of the moraine ridge. The sampled sediments are dominated by supraglacial sediments, which are more extended to reset prior to depositions (Ou et al, 2014; Richards 2000; Tsukamoto et al. 2002). Sample BDO-6 was collected from the lower part of the QM3 ridge, where the source of the debris is more complicated and may have consisted of mixted deposits, and probably caused poor bleaching. In addition, previous studies show that the original OSL signal of some quartz could weaken by 1% after 10 s exposure under natural light (Aitken 1998); in high-altitude regions, the high angle of solar radiation and increase in UV flux with elevation makes bleaching of the signal from quartz easier (Aitken 1998). As Qinggulong is located in southeastern QTP at an altitude > 4300 m, there is very limited time, prior to burying, for total bleaching of the quartz signal from moraines found on the ridge top.

The silt used for ESR was collected from JM3 and JM4 of glaciofluvial sediments in the Juequ Valley. Owing to the greater transport distance between the glacier margin and point of deposition, which increases the probability of grains having sufficient exposure to sunlight, glaciofluvial sediments are considered more likely to have been bleached than those within glacial landforms (Thrasher et al. 2009). The Ti centre ESR signal is more suitable than others for the ESR dating of Quaternary sediment (Liu et al. 2010, 2011; Rink et al. 2007; Tissoux et al. 2008). Several experiments claimed that Ti-Li centres can be completely bleached within several to dozens of hours when exposed to sunlight or UV light in different situations (Liu et al. 2013; Tanaka et al. 1997; Tissoux et al. 2007; Voinchet et al. 2007). The results of natural sunlight bleaching of the Ti centre in quartz extracted from granite at different altitudes shows that the necessary time for the Ti centre signal to be bleached to zero decreases as the altitude increases (Gao et al. 2009). High altitude conditions meet the requirements for illumination and ultraviolet intensity by signals from quartz Ti-Li centres (Gao et al. 2009), and are considered the best locations for sampling. The Ti-Li centre ESR dating results correspond with the other dating method results on aqueous sediment, aeolian sediment, and mixed sediment (Liu et al, 2016). The dating samples JQE-01, JQE-02, and JQE-03 were collected from glaciofluvial sediments at higher elevation. Therefore, the ESR signals of the Ti-Li centres in glacial quartz grains could be removed. The dating results are consistent with the morphological relationship; previous studies have shown that Ti-Li centre ESR signal dating results are reliable and credible, and that this technique can be applied to Quaternary glaciation research of moraines and terraces (Zhang and Chai 2016; Zhang et al. 2017).

5.2 Glacial history of the Tayantaweng Shan

The results of this field survey and dating results show that the ESR and OSL contribute new data for a temporal framework displaying a long and complex history of landscape evolution in the middle section of the Tayantaweng Shan.

The terminal moraine samples (JQE-02, JQE-03) from JM4 in the Juequ Valley were ESR-dated to 212 ± 21.34 ka and 240.3 ± 49.8 ka, respectively, corresponding to MIS 6, and showed good agreement with the ESR dating results (192 ± 51 ka - 207 ±45 ka) in the Quzha Valley. Moraine QM4 in the Ruqu Valley may also have formed during this period. Glaciofluvial deposits (JQE-01) from the terminal moraine JM3 in the Juequ Valley were

ESR-dated to 51.78 ± 10.62 ka, corresponding to MIS 3, in accordance with the fourth group moraines (QM4) of Qinggulong Village, and were dated by ESR as 55 ± 8 ka and 54 ± 9 ka. The dating result of moraine BDO-4 from the lower lateral side (QM 2) was 17.3 ± 1.25 ka, correspond to the late glacial. The dating results of moraines BDO-5 and BDO-6 from the higher lateral side (QM 3) (31.38 ± 3.48 ka and 25.78 ± 1.98 ka, respectively) agree with the ESR results (38 ± 6 ka, 31 ± 6 ka, 26 ± 4 ka, and 25 ± 1 ka), which suggests that the moraines formed during the LGM and correspond to MIS 2 (Zhang and Chai 2016). The cirque contains the least amount of moraine (QM1), which is determined to be from the Neoglaciation / Little Ice Age based on relative geomorphology, and corresponds to MIS 1.

5.3 Comparison with glaciation in neighbouring mountains

Our glacial chronology derived using ESR and OSL datings in the middle section of the Tayantaweng Shan is consistent with glacial chronologies in nearby mountain ranges, the Hengduan Mountains and the southeastern Tibetan Plateau. This is confirmed by our five ESR ages of (192 ± 51)-(240.3 ± 49.8) ka (MIS 6) from the Quzha Valley and Juequ Valley. The MIS 6 glacial advance is apparently the earliest glaciation recorded with numerical ages in this area. During this period, the glaciers in the Quzha Valley, Juequ Valley, and Ruqu Valley advanced approximately 16–35 km down- valley and reached elevations of 4300-4800 m a.s.l. It was determined that the glacier extent in the valleys on the side of the Yuqu river had generally reached valley mouths during the maximum glaciation period. There is a comparatively high glaciofluvial terrace in the upper reaches of Yuqu River; it is approximately 30 m in height, with might be appropriate to the MIS 6 glacial advance (Yang et al. 1983).

There is an obvious difference with respect to the extent of different glaciations in both the Hengduan Mountains and southeastern QTP (Figure 11). In several adjacent mountains with absolute chronological data, the dating results of the Shaluli Shan (Fu et al. 2014), Daocheng (Zheng and Ma 1995), Baimaxue Shan (Zhang et al. 2015), Yulong Mountain (Zheng, 2000; Zhao et al. 1999), and Nyainqêntanglha Mountain (Zhao et al. 2002) show preserved moraines from the Zhonglianggan glaciation (corresponding to MIS 12), the Kunlun glaciation (corresponding to MIS 16/18), when glaciers reached their maxima. On the other hand, the initial glaciation in the Gongga Mountains (Wang et al. 2013) and Tanggula Mountains (Owen et al. 2005; Wang et al. 2007), as in the middle section of the Tayantaweng Shan, was the penultimate glaciation (MIS 6). All these areas are influenced by the southwest monsoon, but there are obvious differences in the timing of maximum glaciation; these possibly correlate to the differences in the time, rate, and amplitude of the tectonic activity in various mountains.

In addition, the Bodui Zangbo was located approximately 130 km from the middle part of the Tayantaweng, and the time of maximum glaciation agrees with Tayantaweng Shan. However, the valley glacier extent reached 100 km during the MIS 6 in this area (Zhou et al. 2010), which was far great than that of Tayantaweng Shan. These two major areas were influenced by the south Asian monsoon. However, there were obvious differences in the glacier extents of the various glacial periods. Precipitation data show a decrease from between approximately 800 to 1000 mm (Bomi) to between approximately 400 to 500 mm (Chang Du) (Li et al. 1986). The spatial variations in glacier extent were possibly caused by spatial differences in precipitation. These findings also indicated that mountain barriers had a clear effect limiting precipitation and thus glacial development in the middle section of the Tayantaweng.

The ESR ages suggest a glacial advance during MIS 3 in the middle section of the Tayantaweng Shan. Glacial advances with similar ages have been reported in the Hengduan Mountains and southeastern QTP, including the Qianhu Mountains (Zhang et al, 2014), Queer Mountains (Xu et al, 2010), Gongga Mountains (Wang et al. 2013), Shaluli Shan (Xu and Zhou 2009), Zheduo Mountains (Xu et al. 2005), and Tanggula Mountains (Wang et a. 2007). From the expanse of the glaciers, the MIS 3 glaciers in these regions are bigger than the MIS 2 glaciers. These features are observed in glacier growth occurring in the same period at the Hengduan Mountains and surrounding mountains (Ou et al. 2014; Wang et al. 2013). A comparative study of pollen data from Rencuo Lake and records of surrounding regions show annual rainfall of only 250 mm during the LGM in southeastern Tibet, which is 40% of what it is today. The climate of the southeastern QTP was also cold; January temperatures were lower by 7-10 ℃ than at present, and July temperatures were 2-5 ℃ lower (Tang et al. 2004). Studies on the pollen of Rencuo Lake and RM core of the Zoige Basin show enlarged desert steppes on the QTP during the LGM, occupying most of the ground and forcing the forests to the southeastern margin (Tang et al. 1998; Shi 2002). A paleoglacial study of the Bodoi Zangbo river basin shows a 6.6 ℃ temperature drop during LGM compared to the present, 40% less precipitation, and a decrease in the ELA by 600 m (Zhou et al. 2010). Based on the above analyses, the Southeastern QTP and Hengduan Mountains are marked by arid and cold weather during the LGM, with violent fluctuations. However, the climate of the eastern and southern QTP during mid-MIS 3 was generally cold and humid under the effects of the south Asian monsoon (Shi and Yao 2002).

6 Conclusions

This study provides conclusive data on the geomorphic features and Quaternary glacial history of the middle section of the Tayantaweng Shan, on the southeastern QTP. The major outcomes of this study are as follows:

Approximately 13000 km^2 was mapped for a geomorphologic map (1:440,000) of Quaternary glaciations. The results showed that typical glacial erosional and depositional landforms were preserved above 4300 m. We present new ESR and OSL chronological ages from glacial landforms. In combination with previous results, we can find that the middle section of Tayantaweng Shan has preserved five stages of glaciations: MIS 6 (192 ± 51 - 240.3 ± 49.8 ka), MIS 3 (51.78 ± 10.62 - 55 ± 8 ka), MIS 2 (25 ± 1 - 38 ± 6 ka), the late stage of the last glacial period (17.3 ± 1.25 ka), all Late Pleistocene, plus the Neoglaciation / Little Ice Age. This glacial chronology is consistent with glacial chronologies from the well-studied Hengduan Mountains and southeastern QTP, which indicates that the timing of Quaternary glaciations across these areas was broadly affected by similar climate.

Glaciation advances during the last glaciation were successively more restricted from MIS 3 to MIS 2, which was perhaps in response to the constant fluctuations in temperature and precipitation in the northern hemisphere during this period. In MIS 2 glaciers in this region were smaller than in MIS 3, probably reflecting the cold and dry climate conditions.

Acknowledgments

This study is supported by the National Natural Science Foundation of China (Nos. 41671005, 41230743, 41501068).

References

Aitken MJ (1998) An introduction to optical dating. Oxford: Oxford University Press.

Arendt A, Bolch T, Cogley JG, et al. (2012) Randolph Glacier Inventory [v2.0]: A dataset of global glacier outlines (Global land ice measurements from space, Boulder Colorado, USA. Digital Media). Retrieved June 10, 2012, from http://www.glims.org/RGI/.

Benn DI, Owen LA (1998) The role of the Indian summer monsoon and the mid-latitude westerlies in Himalayan glaciation: Review and speculative discussion. Journal of the Geological Society 155(2): 353-363. https://doi.org/10.1144/gsjgs.155.2.0353

Benn DI, Owen LA (2002) Himalayan glacial sedimentary environments: a framework for reconstructing and dating the former extent of glaciers in high mountains. Quaternary International 97(3): 3-25. https://doi.org/10.1016/S1040-6182(02)00048-4

Bi WL, Yi CL (2016) Review of ESR dating technique in Quaternary glacial chronology. Journal of Glaciology and Geocryology 38(5): 1292-1299 (in Chinese). https://doi.org/110.7522/j.issn.1000-0240.2016.0151

Cui ZJ, Chen YX, Zhang W, et al. (2011) Research History, glacial chronology and origins of Quaternary glaciations in China. Quaternary Sciences 31(5): 749-764 (in Chinese). https://doi.org/10.3969/j.issn.1001-7410.2011.05.01

Dortch JM, Owen LA, Caffee MW (2013) Timing and climatic drivers for glaciation across semi-arid western Himalayan-Tibetan orogen. Quaternary Science Reviews 78(11): 188-208. https://doi.org/10.1016/j.quascirev.2013.07.025

Fu P, Heyman J, Hättestrand C, et al. (2012) Glacial geomorphology of the Shaluli Shan area, southeastern Tibetan Plateau. Journal of Maps 8(1): 48-55. https://doi.org/10.1080/17445647.2012.668762

Fu P, Stroeven AP, Harbor JM, et al. (2014) Paleoglaciation of Shaluli Shan, southeastern Tibetan Plateau. Quaternary Science Reviews 64(433): 121-135. https://doi.org/10.1016/j.quascirev.2012.12.009

Fuchs M, Owen LA (2008) Luminescence dating of glacial and associated sediments: review, recommendations and future directions. Boreas 37, 636–659. https://doi.org/10.1111/j.1502-3885.2008.00052.x

Gao L, Ying GM, Liu CR, et al. (2009) Nature sunlight bleaching of Ti center ESR signal in quartz. He Jishu/Nuclear Techniques 32(2): 116-118.

Lai ZP (2010) Chronology and the upper dating limit for loess samples from Luochuan section in Chinese Loess Plateau using quartz OSL SAR protocol. Journal of Asian Earth Sciences 37, 176-185. https://doi.org/10.1016/j.jseaes.2009.08.003

Lehmkuhl F, Owen LA (2005) Late Quaternary glaciation of Tibet and the bordering mountains: a review. Boreas 34(2): 87–100. https://doi.org/10.1111/j.1502-3885.2005.tb01008.x

Li JJ, Zheng BX, Yang XJ, et al. (1986) The series of the scientific expedition to Qinghai-Xizang Plateau. Science Press, Beijing (in Chinese).

Li JJ (1991) The environmental effects of the uplift of the Qinghai-Xizang Plateau. Quaternary Science Reviews 10(6): 479-483. https://doi.org/10.1016/0277-3791(91)90041-R

Lindholm MS, Heyman J (2015) Glacial geomorphology of the Maidika region, Tibetan Plateau. Journal of Maps 12: 1-7. https://doi.org/10.1080/17445647.2015.1078182

Liu GN, Li YK, Chen YX, et al. (2011) Glacial landform chronology and environment reconstruction of Peiku Gangri.

Himalayas. Journal of Glaciology and Geocryology 33: 959-970. (in Chinese)

Liu CR, Yin GM, Grün R (2013) Research Progress of the Resetting Features of Quartz ESR Signal. Advances in Earth Science 28(1):24-30.

Liu CR, Yin GM, Gao L, et al. (2011) Research advances in ESR geochronology of Quaternary deposits. Seismology and Geology 2(33): 490-498. https://doi.org/10.3969/j.issn.0253-4967.2011.02.022

Liu C R, Yin G M, Gao L, et al. (2010) ESR dating of Pleistocene archaeological localities of the Nihewan Basin, North China - Preliminary results. Quaternary Geochronology 5(2): 385-390. https://doi.org/10.1016/j.quageo.2009.05.006

Liu CR, Yin GM, Han F, et al. (2016) ESR dating methodology and its application in dating Quaternary terrestrial sediments. Quaternary Sciences 36(5): 1236-1245. https://doi.org/10.11928/j.issn.1001-7410.2016.05.18

Liu BB, Zhang W, Cui ZJ, et al. (2015) Climate-tectonics coupling effect on Late Quaternary Glaciation in the Mayaxue Shan , Gansu Province. Journal of Glaciology and Geocryology 37(3): 701-710. https://doi.org/10.7522/j.issn.1000-0240.2015.0079

Lisiecki, LE, Raymo, ME (2005) A Pliocene-Pleistocene stack of 57 globally distributed benthic $\delta^{18}O$ records. Paleoceanography 20, PA1003. https://doi.org/10.1029/2004PA001071

Murray AS, Wintle AG (2000) Luminescence dating of quartz using an improved single-aliquot regenerative-dose protocol. Radiation Measurements 32: 57-73. https://doi.org/10.1016/S1350-4487(99)00253-X

Norton KP, Abbuhl LM, Schlunegger F (2010) Glacial conditioning as an erosional driving force in the Central Alps. Geology 38(7): 655-658. https://doi.org/10.1130/G31102.1

Ou XJ, Lai ZP, Zhou SZ, et al. (2014) Timing of glacier fluctuations and trigger mechanisms in eastern Qinghai-Tibetan Plateau during the late Quaternary. Quaternary Research 81(3): 464-475. https://doi.org/10.1016/j.yqres.2013.09.007

Owen LA, Finkel RC, Barnard PL, et al. (2005) Climatic and topographic controls on the style and timing of late Quaternary glaciation throughout Tibet and the Himalaya defined by ^{10}Be cosmogenic radionuclide surface exposure dating. Quaternary Science Reviews 24: 1391-1411. https://doi.org/10.1016/j.quascirev.2004.10.014

Owen LA, Finkel RC, Haizhou M, et al. (2003) Timing and style of Late Quaternary glaciation in northeastern Tibet. Geological Society of America Bulletin 115(11): 1356. https://doi.org/10.1130/B25314.1

Owen LA, Dortch JM (2014) Nature and timing of Quaternary glaciation in the Himalayan-Tibetan orogen. Quaternary Science Reviews 88(88): 14-54. https://doi.org/10.1016/j.quascirev.2013.11.016

Owen LA, Robinson R, Benn DI, et al. (2009) Quaternary glaciation of Mount Everest. Quaternary Science Reviews 28: 1412–1433. https://doi.org/10.1016/j.quascirev.2009.02.010

Prescott JR, Hutton JT (1994) Cosmic-ray contributions to dose-rates for luminescence and ESR dating - large depths and long-term time variations. Radiation Measurements 23: 497-500. https://doi.org/10.1016/1350-4487(94)90086-8

Richards B (2000) Luminescence dating of Quaternary sediments in the Himalaya and High Asia: A practical guide to its use and limitations for constraining the timing of glaciation. Quaternary International 65(99): 49-61. https://doi.org/10.1016/S1040-6182(99)00036-1

Rink WJ, Bartoll J, Schwarcz HP, et al. (2007) Testing the reliability of ESR dating of optically exposed buried quartz sediments. Radiation Measurements 42(10):1618-1626. https://doi.org/10.1016/j.radmeas.2007.09.005

Shi YF, Huang MH, Ren BH (1988) An introduction to the glaciers in China contents. Science Press, Beijing (in

Chinese).

Shi YF, Liu SY (2000) Estimation on the response of glaciers in China to the global warming in the 21st century. Chinese Science Bulletin 45 (7): 668-672. https://doi.org/10.1007/BF02886048

Shi YF, Yao TD (2002）MIS 3b (54-44 ka BP) cold period and glacial advance in middle and low latitudes. Journal of Glaciolgy & Geocryology 24(1): 1-9. https://doi.org/10.3969/j.issn.1000-0240.2002.01.001

Shi,YF (2002) Characteristics of late Quaternary monsoonal glaciation on the Tibetan Plateau and in East Asia. Quaternary International 97-98: 79-91. https://doi.org/10.1016/S1040-6182(02)00053-8

Su Z, Pu JC (1996) Development conditions, Number and morphological characteristics of glaciers in the Hengduan Mountains region. In: Li JJ, Su, Z 1996. Glaciers in the Hengduan Mountains. Science Press, Beijing, pp. 1-21 (in Chinese).

Tanaka K, Hataya R, Spooner NA, et al. (1997) Dating of marine terrace sediments by ESR, TL and OSL methods and their applicabilities. Quaternary Science Reviews 16(3-5): 257-264. https://doi.org/10.1016/S0277-3791(96)00092-3

Tissoux H, Toyoda S, Falguères C, et al. (2008) ESR dating of sedimentary quartz from two Pleistocene deposits using Al and Ti-Centers. Geochronometria 30(-1): 23-31. https://doi.org/10.2478/v10003-008-0004-y

Tissoux H, Falguères C, Voinchet P, et al. (2007) Potential use of Ti-center in ESR dating of fluvial sediment. Quaternary Geochronology 2(1): 367-372. https://doi.org/10.1016/j.quageo.2006.04.006

Tang LY, Shen CM, Liu KB, et al. (2004) Climatic changes since the Last Glacial Maximum in the southeastern Tibetan Plateau: pollen evidence. Science in China 34(34): 434-442. (in Chinese)

Tang LY, Shen CM, Kong ZZ, et al. (1998) Pollen evidence of climate during the Last Glacial Maximum in eastern Tibetan Plateau. Journal of Glaciology and Geocryology 20(2): 133-140. (in Chinese)

Thrasher IM, Mauz B, Chiverrell RC, et al. (2009) Luminescence dating of glaciofluvial deposits: a review. Earth Science Reviews 97: 133-146. https://doi.org/10.1016/j.earscirev.2009.09.001

Tschudi S, Schafer JM, Zhao ZZ, et al. (2003) Glacial advances in Tibet during the younger dryas? Evidence from cosmogenic ^{10}Be, ^{26}Al, and ^{21}Ne. Journal of Asian Earth Sciences 22: 301-306. https://doi.org/10.1016/S1367-9120(03)00035-X

Tsukamoto S, Asahi K, Watanabe T, et al. (2002) Timing of past glaciations in Kanchenjunga Himal, Nepal by optically stimulated luminescence dating of tills. Quaternary International 97(02): 57-67. https://doi.org/10.1016/S1040-6182(02)00051-4

Voinchet P, Falguères C, Tissoux H, et al. (2007) ESR dating of fluvial quartz: Estimate of the minimal distance transport required for getting a maximum optical bleaching. Quaternary Geochronology 2(1): 363-366. https://doi.org/10.1016/j.quageo.2006.04.010

Wang J, Pan BT, Zhang GL, et al. (2013) Late Quaternary glacial chronology on the eastern slope of Gongga Mountain, eastern Tibetan Plateau, China. Science China: Earth Sciences 56 (3): 354-365. https://doi.org/10.1007/s11430-012-4514-0

Wang J, Zhou SZ, Tang SL, et al. (2007) The Sequence of Quaternary glaciations around the Tanggula Pass. Journal of Glaciology and Geocryology 29(1): 149-155. https://doi.org/10.3969/j.issn.1000-0240.2007.01.023

Xu LB，Zhou SZ, Wang J (2005) Pleistocene glaciations in the Shaluli Shan and the influences of southwest monsoon on the glaciations during the last glacial period . Quaternary Sciences 25 (5): 620-629. (in Chinese) https://doi.org/10.3321/j.issn:1001-7410.2005.05.011

Xu LB，Zhou SZ (2009) Quaternary glaciations recorded by glacial and fluvial landforms in the Shaluli Mountains, South Eastern Tibetan Plateau. Geomorphology 103: 268-275. https://doi.org/10.1016/j.geomorph.2008.04.015

Xu LB, Ou XJ, Lai ZP, et al. (2010) Timing and style of Late Pleistocene glaciation in the Queer Shan, northern Hengduan Mountains in the eastern Tibetan Plateau. Journal of Quaternary Science 25(6): 957-966. https://doi.org/10.1002/jqs.1379

Yang YC, Li BY, Yin ZS, et al. (1983) Geomorphology of Xizang. Science Press, Beijing, pp. 92-95 (in Chinese).

Yi CL, Bi WL, Li JP (2016) ESR dating of glacial moraine deposits: Some insights about the resetting of the germanium (Ge) signal measured in quartz. Quaternary Geochronology 35:69-76. https://doi.org/10.1016/j.quageo.2016.06.003

Yokoyama Y, Falgueres C, Quaegebeur JP (1985) ESR dating of quartz from quaternary sediments: First attempt. Nuclear Tracks & Radiation Measurements 10(4): 921-928. https://doi.org/10.1016/0735-245X(85)90109-7

Zhang W, Bi WL, Liu BB, et al. (2015) Geochronology constrainted on late Quaternary glaciation of Baimaxue Shan. Quaternary Sciences 35(1): 20-37 (in Chinese). https://doi.org/10.11928/j.issn.1001-7410.2015.01.03

Zhang W, Chai L (2016a) The preliminary study of the Quaternary glacier in middle part of the Tenasserim Chain with ESR dating method. Journal of Glaciology and Geocryology 38(5): 1281-1291. (in Chinese) https://doi.org/1000-0240.2016.0150

Zhang W, Cui ZJ, Li YH (2016b) Quaternary glacial development and mechanism in the eastern margin of the Qinghai Tibet Plateau. Da Lian Maritime University Press, Dalian, pp. 1-104. (in Chinese)

Zhang W, Liu BB, Li YH, et al. (2014) Late Pleistocene glaciations on Qianhu Mountain, northwest Yunnan Province, China. Geografiska Annaler Series A: Physical Geography 96(3): 417-429. https://doi.org/10.1111/geoa.12041

Zhang W, Liu L, Chai L, et al. (2017) Characteristics of Quaternary glaciations using ESR dating method in the Luoji Mountain, Sichuan Province. Quaternary sciences 32(2): 281-292. (in Chinese) https://doi.org/10.11928/j.issn.1001-7410.2017.02.07

Zhao XT, Qu YX, Li TS (1999) Pleistocene glaciation along the eastern foot of the Yulong Mountains. Journal of Glaciology and Geocryology 21(3): 242-248.

Zhao XT, Wu ZH, Zhu DG, et al. (2002) Quaternary glaciation in the west Nyaiqentanglha Mountains. Quaternary sciences 22(5): 424-433. (in Chinese) https://doi.org/10.3321/j.issn:1001-7410.2002.05.004

Zheng BX (2000) Quaternary glaciation and glacier evolution in the Yulong Mount, Yunnan. Journal of Glaciology and Geocryology 22(1): 53-61. (in Chinese)

Zheng BX, Ma QH (1995) A Study on the Geomorphological Characteristics and Glaciations in Paleo-Daocheng Ice Cap, Western Sichuan. Journal of Glaciology and Geocryology 17(1): 23-32. (in Chinese)

Zhou SZ, Wang J, Xu LB, et al. (2010) Glacial advances in southeastern Tibet during late Quaternary and their implications for climatic changes. Quaternary International 218(1): 58-66. https://doi.org/10.1016/j.quaint.2009.11.026

Figures

Fig1. Overview map of the Tibetan Plateau showing the location of the Tayantaweng Shan in the southeastern part of the Tibetan Plateau. The glaciers (white) are based on Arendt et al. (2012) with minor updates. 1. Gongga Mountain; 2. Queer Shan; 3. Daocheng; 4. Yulong Mountain; 5. Qianhu Mountain; 6. Baima Mountain; 7. Tayantaweng Shan; 8. Nyaiqentanglha; 9. Tanggula; 10. Mayaxue

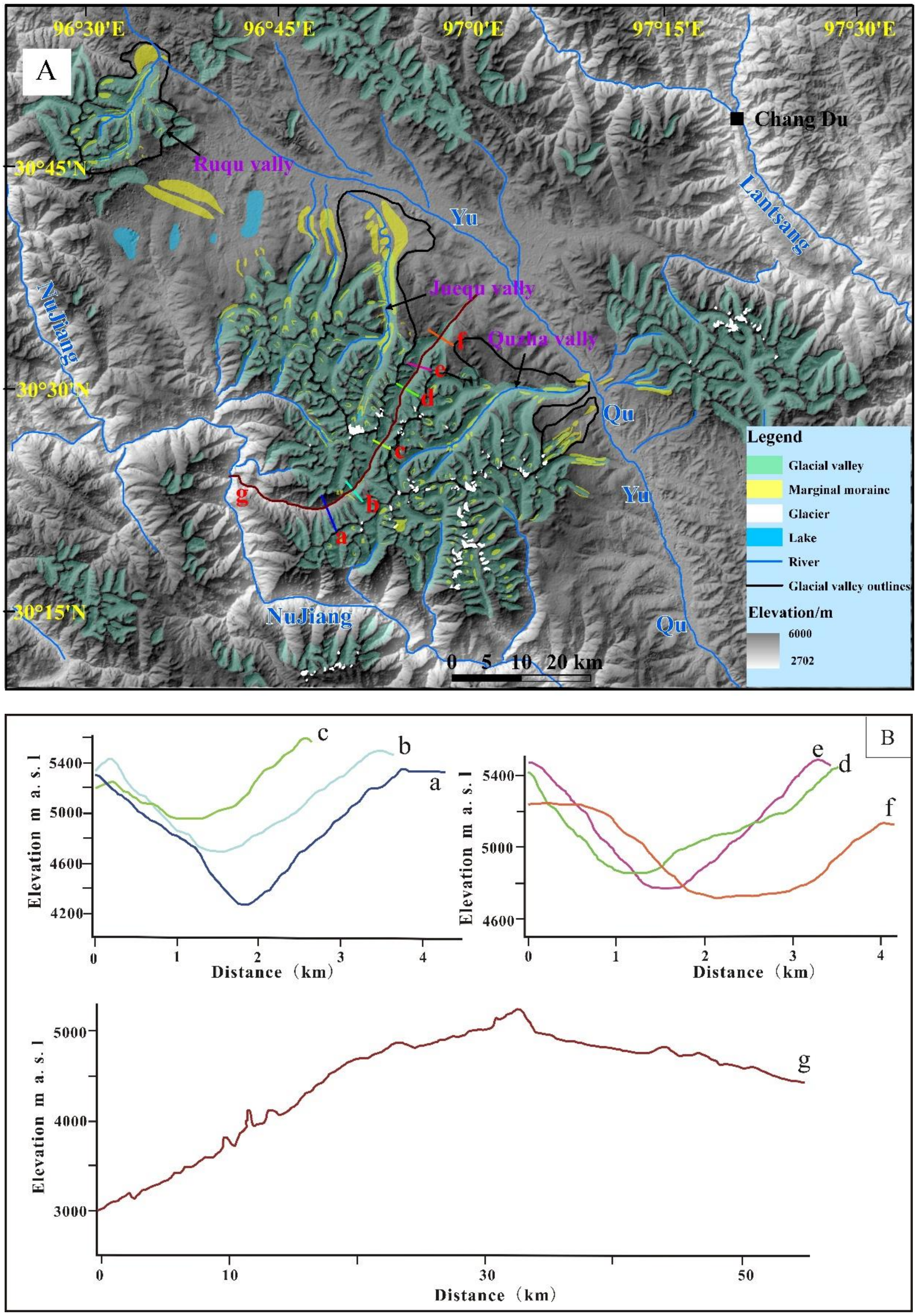

Shan; 11. Anyemaqen Mountain

Figure 2. (A) Distribution of glacial deposits, glacial geomorphology and the track of the field valley; (B)

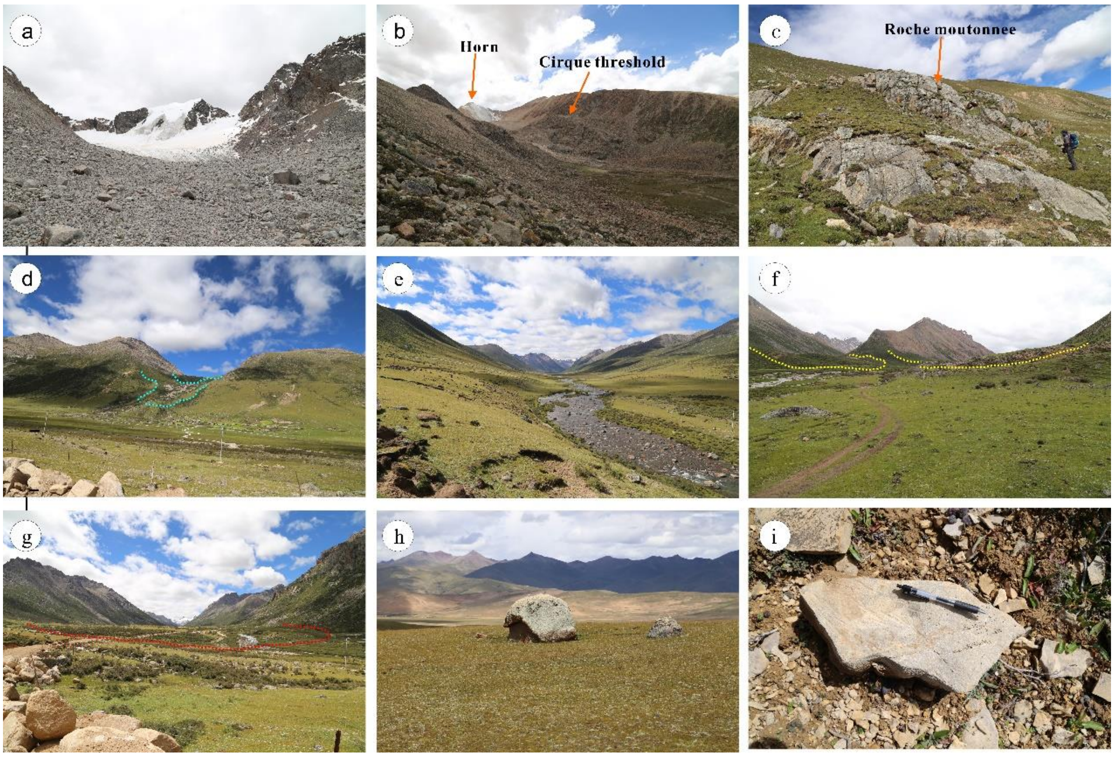

Transverse valley profiles (upper panels) and longitudinal valley profile (lower panel).

Figure 3. Field photographs showing: a) Contemporary glacier and front deposits in the source of the Quzha Valley; b) Internal terminal moraine QM1, cirque threshold, and horn in the cirque above Qinggulong Village; c) Roche moutonnée at the high lateral moraine of the Ruqu Valley; d) Hanging valley in the Juequ Valley and deposits at valley mouth; e) Juequ U-type valley, and moraine ridge at both sides (JM4); f) Terminal moraine, moraine platform, and arête at the intersection location of the upstream trough valley of the Zhaqu Valley; g) JM3 terminal moraine in the Juequ Trough Valley; h) Severely weathered granite gravel on the crest of the terminal moraine JM4 at the valley mouth of the Juequ Valley; i) Moraine and surface scratches on the crest of the terminal moraine RM4 at the mouth of the Ruqu Valley.

Figure 4. Glacial deposit distribution of the (A) Quzha Valley; (B) Juequ Valley; (C) Ruqu Valley.

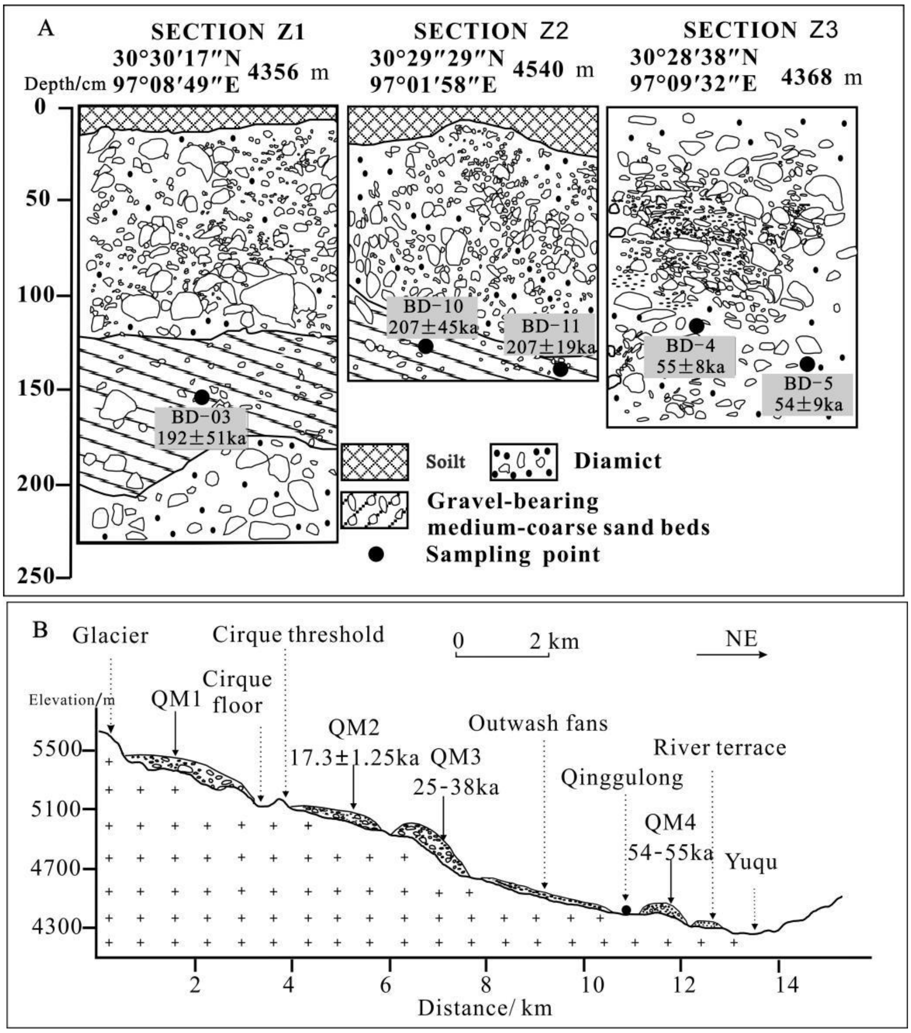

Figure 5. (A) Sediment characteristic diagrams and ESR sampling point for Quzha Valley and Qinggulong Village (Zhang and Chai 2016); (B) Longitudinal section of the Qinggulong Village.

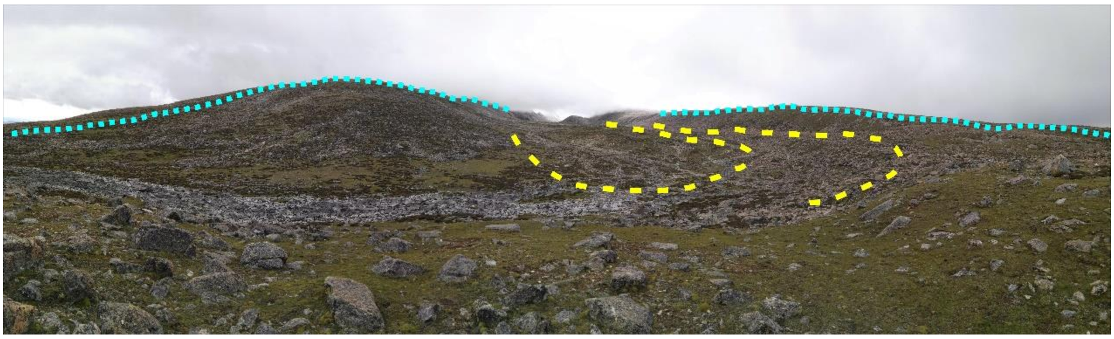

Figure 6. Upper QM2 moraine (yellow line) and QM3 moraine ridge (blue line) in Qinggulong Village,

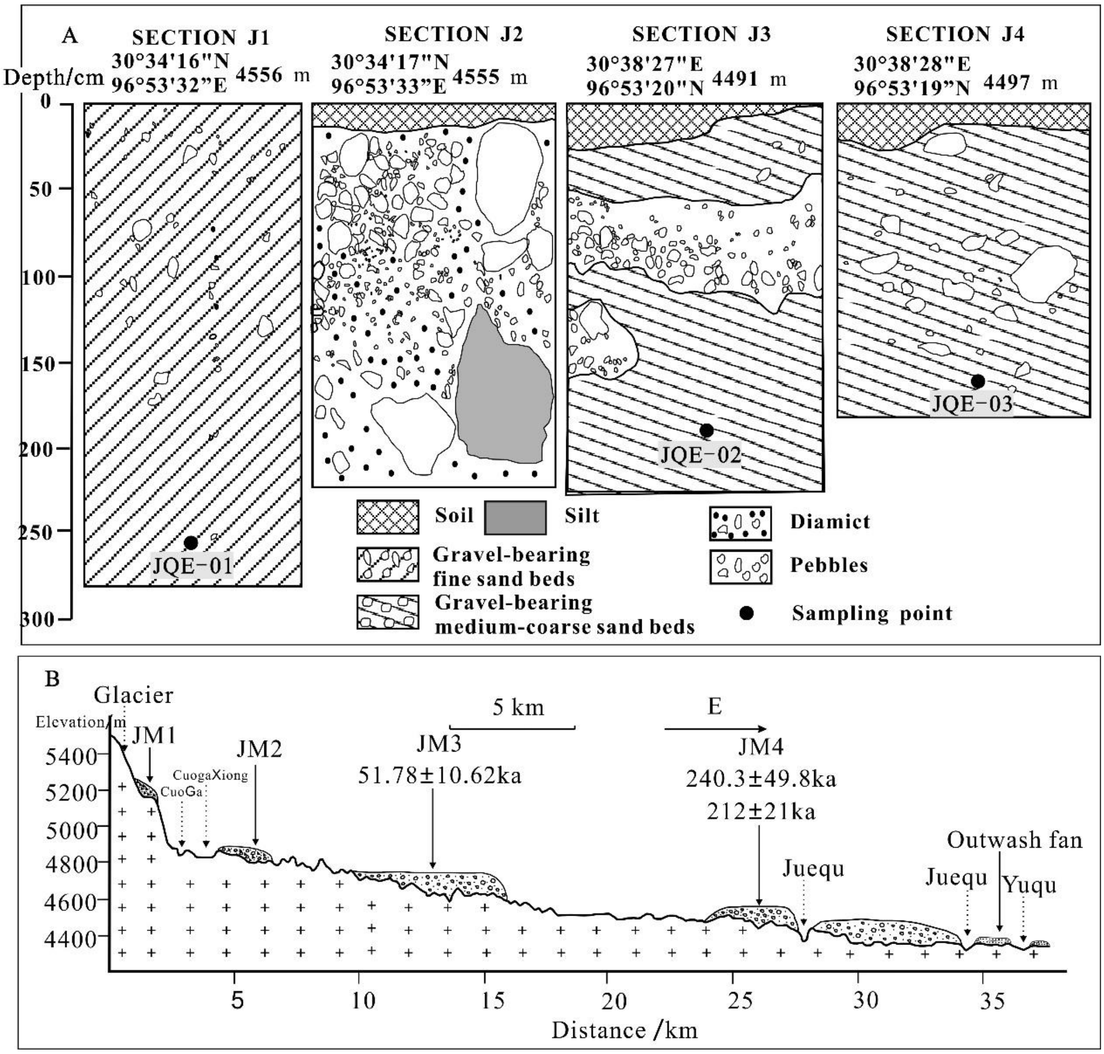

as viewed from the crest of the QM3 terminal moraine.

Figure 7. (A) Sediment characteristic diagrams and ESR sampling point for Juequ valley; (B) Longitudinal section of the Quaternary glacial landforms in the Juequ Valley.

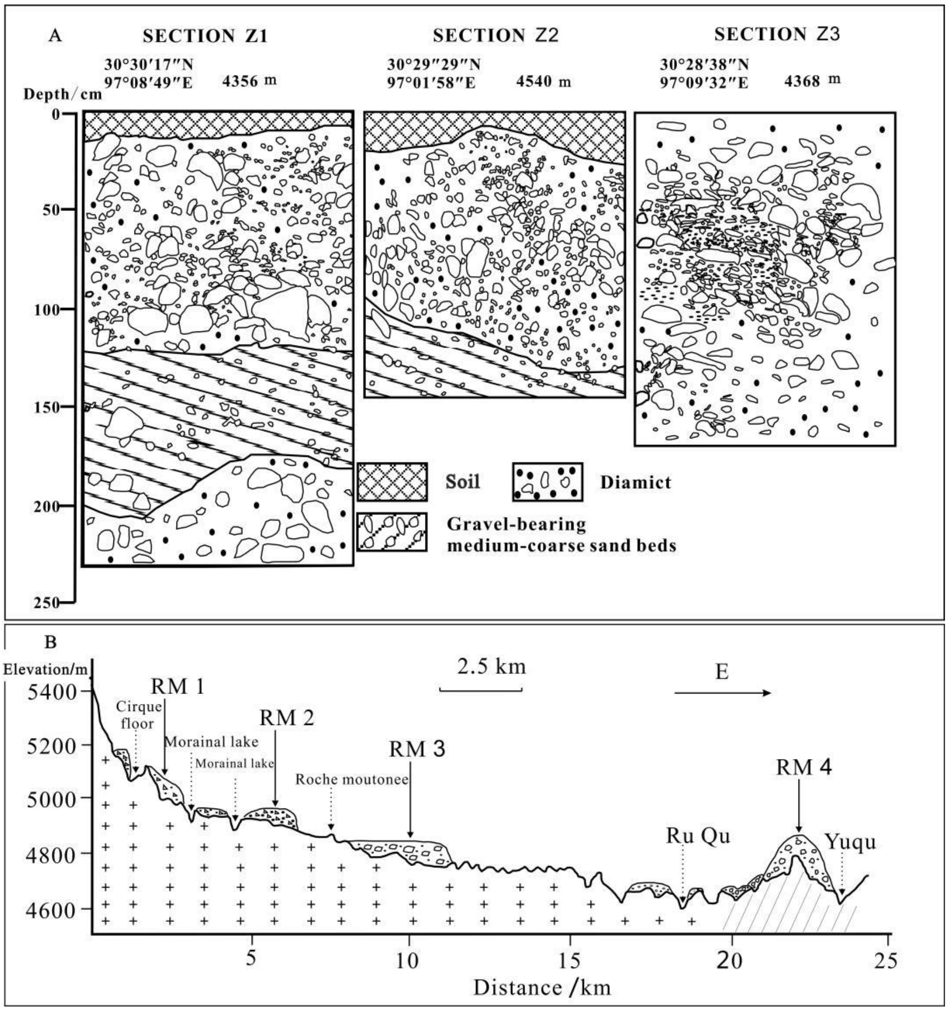

Figure 8. (A) Sediment characteristic diagrams for Ruqu valley; (B) Longitudinal section of the Quaternary glacial landforms in the Ruqu Valley.

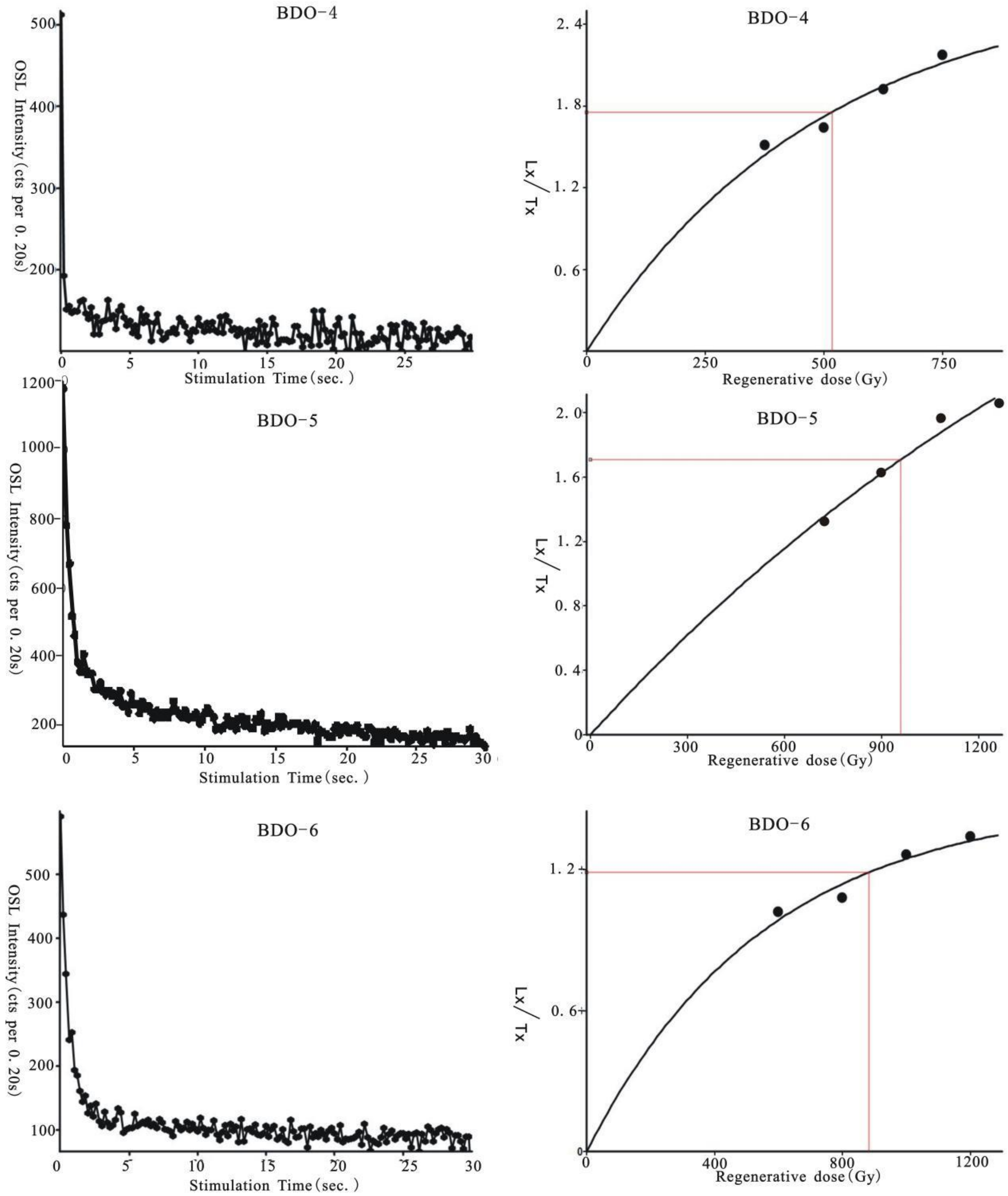

Figure 9. Representative data of De determination by the sensitivity-corrected MAR protocol. Decay curves of natural and regeneration dose OSL intensity (Li) and the corrected OSL (Li/Ti) dose-response curves and De determination.

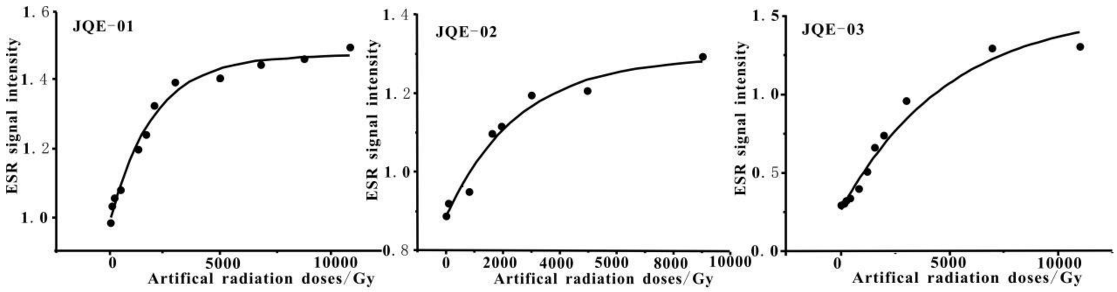

Figure 10. Relations between ESR intensity and irradiation dose of the samples from the Tayantaweng Shan.

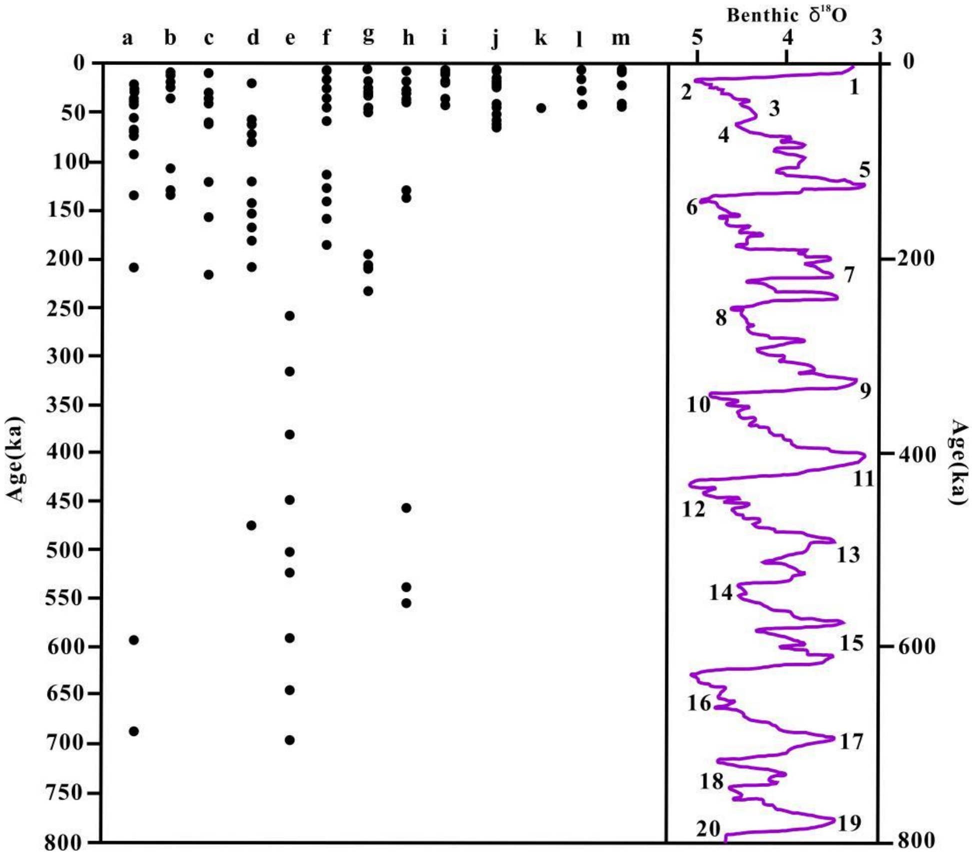

Figure 11. Glacial chronology data from different mountain areas: a. Nyaiqentanglha (Zhao et al. 2002); b. Bomi (Zhou et al. 2010); c. Tanggula (Owen et al. 2005; Wang et al. 2007); d. Baimaxue Shan (Zhang et al. 2015); e. Yulong Mountain (Zheng 2000); f. Gongga Mountain (Wang et al. 2013); g. Tayantaweng Shan; h. Shaluli Mountain (Xu et al. 2009); i. Qianhu Mountain (Zhang et al. 2014); J. Queer Shan (Xu et al. 2010); K. Zheduo Mountain (Xu et al. 2005); l. Anyemaqen Mountain (Owen 2003); m. Mayaxue Shan (Liu et al. 2015). Stacked marine $\delta^{18}O$ curves of Lisiecki and Raymo (2005).

Tables

Table 1. OSL dating results in the Qinggulong valley

OSL Number	Elevation /m	Position	Depth (m)	Samples	U /ppm	Th /ppm	K (%)	Water content /%	Dose rate GY/Ka^{-1}	De /GY	Dating /ka
BDO-4	4644	97°08′19.99″E 30°27′05.12″N	0.65	siltti l	2.56	12	1.54	0.59	3.428	59.3±4.3	17.3±1.25

BDO-5	4867	97°08′04.04″E 30°26′35.42″N	0.7	silttil	2.8	12.9	1.47	0.93	3.476	109.06± 12.1	31.38±3.48
BDO-6	4922	97°07′44.36″E 30°26′34.54″N	1.0	silttil	2.83	13	1.71	3.8	3.645	93.97±7. 2	25.78±1.98

Table 2. ESR dating results as well as the correlated parameters in the Tayantaweng Shan

ESR Number	Elevation /m	Position	Samples	Depth /m	U μg/g^{-1}	Th μg/g^{-1}	Ka μg/g^{-1}	Water content %	De /Gy	Dose rate GY/Ka^{-1}	age /ka
JQE-01	4598	96°53′32.″E 30°38′16″N	silt	2	9.29	105	3.63	2.6	701±143	13.53	51.78±10.62
JQE-02	4506	96°53′33.″E 30°38′04″N	silt	0.8	7.52	84.1	4.17	1.7	2977±585	12.38	240.3±49.8
JQE-03	4491	96°53′19.″E 30°38′29″N	silt	1.2	6.36	62.5	4.24	2.05	2258±226	10.61	212±21

Publications, 1995 - 2018 (chronological order) **Dr. Ian S. Evans, Durham University**

***f = File available** (including all after 2009)

***f Evans, I. S.** & Cox, N. J. 1995 The form of glacial cirques in the English Lake District, Cumbria. *Zeitschrift für Geomorphologie, N.F.* 39, 175-202

***f Evans, I. S.** & McClean, C. J., 1995 The land surface is not unifractal; variograms, cirque scale and allometry. *Zeitschrift für Geomorphologie, N.F. Supplement-Band* 101, 127-147

***f Evans, I. S.** 1996 Abraded rock landforms (whalebacks) developed under ice streams in mountain areas. *Annals of Glaciology* 22, 9-16 (Glacial erosion & Sedimentation)

Evans, I. S. 1997 Process and form in the erosion of glaciated mountains. *In* Stoddart, D.R. (ed.) *Process and form in geomorphology*. Festschrift for Richard J. Chorley. 145-174. Routledge, London.

***f Evans, I. S.** 1997 Cirques and moraines of the Helvellyn Range, Cumbria: Grisedale and Ullswater. Ch. 3.0, 63-87 *in* J. Boardman (ed.) *Geomorphology of the Lake District: a field guide*. British Geomorphological Research Group, Oxford.

Kumar, N. & E**vans, I. S.** 1997 Map output format from GIS: optimising visual quality of paper and electronic atlases. *Cartographic Journal* 34 (1), 37-41

Evans, I. S. 1998, in Goudie, A. S. (ed.) Translation of 1990 *Geomorphological Techniques* into German as *Geomorphologie: Ein Methodenhandbuch für Studium und Praxis*. Two chapters by ISE: General Geomorphometry, *Allgemeine Geomorphometrie*, 45-59 and Cartographic Techniques in Geomorphology, *Geomorphologische Kartierung*, 106-119; plus consolidated references. Berlin: Springer. ISBN 3-540-62905-X.

Evans, I. S. 1998 What do terrain statistics really mean? Ch.6, 119-138 *in* Lane, S.N., Richards, K.S., & Chandler, J.H. (eds.) *Landform monitoring, modelling and analysis.* J.Wiley, Chichester. ISBN 0-471-96977-X

***f Evans, I. S.** & Cox, N J. 1999 Relations between land surface properties: altitude, slope and curvature. *In* Hergarten, S. and Neugebauer, H.J. (eds.) *Process modelling and landform evolution*, 13-45. Lecture Notes in Earth Sciences, 78. Springer, Berlin. ISBN 3-540-64932-8

Evans, I. S. 1999 Castle Eden Dene and Blunts Dene. *In* Bridgland, D.R., Horton, B.P. & Innes, J.B. (eds.) *The Quaternary of North-east England: Field Guide*, 57 – 64 (plus references). London: Quaternary Research Association. ISSN 0261 3611

***f Evans, I. S.** 1999 Was the cirque glaciation of Wales time-transgressive or not? *Annals of Glaciology*, 28, 33-39.

Raju, S., Atkins, P.J., Kumar, N., Townsend, J.G. in collaboration with Corbridge, S., Duvvury, N., **Evans, I**., Harriss, B., Kumar, S. & Oughton, E.A. 1999 *Atlas of Women and men in India*. 131 pp. Kali for Women, New Delhi: for Department for International Development. ISBN: 81-85107-94-7

Evans, I. S. 2000 Active Margin, Factor of safety, Fan delta, Force, Fractal, Headwall, Resistance, Rifting, River terrace, Supercontinent: *entries in* Goudie, A.S., Thomas, D. *et al*. (eds.) *Dictionary of Physical Geography*, 3rd. edition. Blackwell's, Oxford.

Evans, Ian 2000 Disappearing glaciers? *Durham University Geographical Society Journal* 2000, 27 - 33

***f** McClean, C. J., & **Evans, I. S.** 2000 Apparent fractal dimensions from continental scale digital elevation models using variogram methods. *Transactions in GIS*, 4(4), 361-378.

Evans, I. S. 2001 Some geomorphometric characteristics of real land surfaces. In Kidner, D.B. & Higgs, G. *GISRUK 2001; Proceedings of the GIS Research UK 9th. Annual Conference*, University of Glamorgan, Wales, 408-410. ISBN 1-840540-26-5

McClean, C. J., & **Evans, I. S.** 2001 Non-fractal behaviour in real land surfaces. In Kidner, D.B. & Higgs, G. *GISRUK 2001; Proceedings of the GIS Research UK 9th. Annual Conference*, University of Glamorgan, Wales, 421-4. ISBN 1-840540-26-5

Evans, I. S. 2001 Scale-specific landforms and aspects of the land surface. In Ohmori, H. (Chief Ed.) *DEMs and Geomorphology (Proceedings of the symposia on New Concepts & Models in Geomorphology, and*

Geomorphometry, DEMs and GIS, 24-26 August 2001, Tokyo). Special Publication of the Geographic Information Systems Association (Tokyo), 22-23 (extended abstract)

McClean, C. J. & **Evans, I. S.** 2001 A further difference between the land surface and Fractional Brownian Surfaces. In Ohmori, H. (Chief Ed.) *DEMs and Geomorphology (Proceedings of the symposia on New Concepts & Models in Geomorphology, and Geomorphometry, DEMs and GIS, 24-26 August 2001, Tokyo)*. Special Publication of the Geographic Information Systems Association (Tokyo), 46-47 (extended abstract)

Arrell, K. E., **Evans I. S.** & Donoghue, D. N. 2002 Using a GIS to predict glacier distributions: considerations when using DEMs (Poster). *Proceedings of the GIS Research UK 10th Annual Conference* GISRUK, University of Sheffield.

Elizabeth Haworth, George de Boer, **Ian Evans**, Henry Osmaston, Winifred Pennington, Alan Smith, Philip Storey & Brian Ware 2003 *'Tarns of the Central English Lake District:* depth surveys and the environmental context.' Ambleside, Cumbria: Brathay Exploration Group Trust. 204 pp. ISBN 0 90601517 0

***f Evans, I. S.** 2003 Lakeland tarns, cirques and glaciation. In Elizabeth Haworth, George de Boer, **Ian Evans**, Henry Osmaston, Winifred Pennington, Alan Smith, Philip Storey, and Brian Ware 2003 *'Tarns of the Central English Lake District:* depth surveys and the environmental context.' Ambleside, Cumbria: Brathay Exploration Group Trust, 9-19 (+refs.).

Arrell, K.E. & **Evans, I. S.** 2003 Viewshed algorithm efficiency: landscape dependant. *GIS Research UK. Proceedings of the 11th Annual Conference* GISRUK. City University, London.

***f** Arrell, K.E. & **Evans, I. S.** 2003 Predicting Glacier Distributions: Local Climate Predictions. *Proceedings, 60th. Annual Eastern Snow Conference*, Sherbrooke, Quebec, Canada.

***f** Schmidt, J., **Evans, I. S.** & Brinkmann, J. 2003 Comparison of polynomial models for land surface curvature calculation. *International Journal of GIS* 17 (8): 797-814.

***f Evans, I. S**. 2003 Scale-specific landforms and aspects of the land surface. In I.S. Evans, R. Dikau, E. Tokunaga, H. Ohmori and M. Hirano (eds.) '*Concepts and modelling in Geomorphology: International Perspectives'*. Tokyo: Terrapub, 61-84.

Evans, I. S., R. Dikau, E. Tokunaga, H. Ohmori and M. Hirano (eds.) 2003 '*Concepts and modelling in Geomorphology: International Perspectives'*. Tokyo: Terrapub, 254 pp.
available on-line at *http://www.terrapub.co.jp/e-library/ohmori/index.html*

***f Evans, I. S.** 2004 Twentieth-Century Change in Glaciers of the Bendor and Shulaps Ranges, British Columbia Coast Mountains. *Quaternary Newsletter*, ISSN 0 143-2826, October 2004, No. 104, pages 70-72. Published by the Quaternary Research Association, London.

Evans, I. S. 2004 'Cirque, glacial' (pp. 154-8) and 'Geomorphometry' (pp. 435-9) in *'Encyclopedia of Geomorphology'*, edited by A. S. Goudie for Int. Assoc. of Geomorphology. London: Routledge, 2 vols., 1184 pages. ISBN 0-415-27298-x

Arrell, K.E, Donoghue, D.N., **Evans, I.S.**, 2005 Fourier Transforms as tool for identifying and removing digital elevation data error *Proceedings of GIS RESEARCH UK 13th Annual Conference* GISRUK. University of Glasgow.

***f Evans, I. S.** & Cox, N. J. 2005 Global variations of local asymmetry in glacier altitude: separation of north-south and east-west components. *Journal of Glaciology* 51 (174), 469-482.

***f Evans, I. S.** 2006a Local aspect asymmetry of mountain glaciation: A global survey of consistency of favoured directions for glacier numbers and altitudes. *Geomorphology* 73 (1-2), 166-184.

***f Evans, I. S.** 2006b Glacier distribution in the Alps: statistical modelling of altitude and aspect. *Geografiska Annaler* 88 A (2), 115-133.

***f Evans, I. S.** 2006c Allometric development of glacial cirque form: geological, relief and regional effects on the cirques of Wales*. Geomorphology* 80 (3-4), 245-266.

***f Evans, I. S.** 2006d Glacial landforms, erosional features: major scale forms. In *ELIAS, S.A. (Ed.) Encyclopedia of Quaternary Science.* Elsevier, Amsterdam, v.1, 838-852. [Evans, D.J.A. (Sub- Ed.) Glacial landforms] [ISBN-10: 0-444-51919-X]

Arrell, Katherine, **Evans, Ian** & Donoghue, Danny 2006
A distributed model for mountain climate and glacier mass balance.

Evans, Ian S. 2007 Glacial cirques of the Brecon Beacons. In Carr, S.J, Coleman, C.G., Humpage, A.J. and Shakesby, R.A. (Eds.); *The Quaternary of the Brecon Beacons: Field Guide.* Quaternary Research association, London, 36-40. [ISBN 0907 780 725]

***f Evans, Ian S.** 2007 Glacier distribution and direction in the Arctic: the unusual nature of Svalbard. *Landform Analysis* 5, 21-24. Association of Polish Geomorphologists, Poznań. [*Extended Abstract, IAG Conference.*]

***f** Minár, Jozef & **Evans, Ian S.** 2008 Elementary forms for land surface segmentation: The theoretical basis of terrain analysis and geomorphological mapping. *Geomorphology* 95 (3-4), 236-259. *doi:10.1016/j.geomorph.2007.06.003. Available online 27 June 2007; published 15 March 2008.*

***f Evans, I. S.** 2008 Glacial erosional processes and forms: mountain glaciation and glacier geography. Ch. 11 In: Burt, T.P., Chorley, R.J., Brunsden, D.., Cox, N.J., & Goudie, A.S (Eds.), *The History of the Study of Landforms or the Development of Geomorphology, v. 4: Quaternary and Recent Processes and Forms (1890-1960s) and the Mid-Century Revolutions.* The Geological Society, London, 413-494. ISBN 978-1-86239-249-6.

Pike, R.J., Hengl, T. & **Evans, I.S.**, 2009 Geomorphometry: A brief guide. Ch. 1 in Hengl, Tomislav. and Reuter, Hannes (eds) Geomorphometry: concepts, software, applications, 3-30. *Developments in Soil Science* 33, Elsevier. Hardbound, £56.99, ISBN-13: 978-0-12-374345-9, 765pages, [SEE *http://www.elsevier.com/wps/find/bookdescription.cws_home/716403/description#description]*

***f all below:**

Hengl, T. & **Evans, I.S.**, 2009 Mathematical and digital models of the land surface. Ch. 2 in Hengl, Tomislav. and Reuter, Hannes (eds) Geomorphometry: concepts, software, applications, 31-63. *Developments in Soil Science* 33, Elsevier. Hardbound, £56.99,
ISBN-13: 978-0-12-374345-9, 765 pages,

Evans, I.S., Hengl, T. & Gorsevski, P. 2009 Applications in geomorphology. Ch. 22 in Hengl, Tomislav. and Reuter, Hannes I. (eds) Geomorphometry: concepts, software, applications, 497-525. *Developments in Soil Science* 33, Elsevier. Hardbound, £56.99, ISBN-13: 978-0-12-374345-9, 765 pages,

Evans, I. S. 2009 A brief report on recent change in small glaciers in British Columbia, Canada. *Quaternary Newsletter*, ISSN 0 143-2826, June 2009, No. 118, pages 28-31. Published by the Quaternary Research Association, London.

Evans, I.S. 2009 Allometric development of glacial cirques: an application of specific geomorphometry. *Extended Abstract for Geomorphometry 2009 Conference Proceedings.* In: Geomorphometry 2009, Edited by R. Purves, S. Gruber, R. Straumann and T. Hengl. University of Zurich, Switzerland, 248-253. *http://geomorphometry.org/Evans2009*

Grant, K.L., Stokes, C.R. & **Evans, I.S.** 2009 Identification and characteristics of surge-type glaciers on Novaya Zemlya, Russian Arctic *Journal of Glaciology* 55 (194), 960-972.

Evans, I.S. & Cox N.J. 2010 Climatogenic north-south asymmetry of local glaciers in Spitsbergen and other parts of the Arctic; *Annals of Glaciology* 51(55), 16-22.

Mîndrescu, M., **Evans, I.S.** & Cox, N.J. 2010 Climatic implications of cirque distribution in the Romanian Carpathians: palaeowind directions during glacial periods. *Journal of Quaternary Research,* 25 (6) 875–888. On-line, February 2010, doi: 10.1002/jqs.1363, 14 pages.

Evans, I.S. 2010 Allometry, scaling and scale-specificity of cirques, landslides and other landforms. *Transactions of the Japanese Geomorphological Union* 31 (2), 133-153. [Invited paper.]

Hengl, T., **Evans, I. S.,** Wilson, J. P., & Gould, M. (eds.) 2011 *Geomorphometry 2011.* Redlands, CA: Geomorphometry.org.

Evans, Ian S. & Minár, Jozef. 2011 A classification of geomorphometric variables. *International Geomorphometry 2011,* Redlands, CA. 105-108. Geomorphometry.org. *http://geomorphometry.org/EvansMinar2011*

Brown Victoria H, Evans David J. A. & **Evans Ian S.** 2011 The glacial geomorphology and surficial geology of the south-west English Lake District. *Journal of Maps* 2011, 221-243.

Evans, Ian S. 2011 Glacier distribution and direction in Svalbard, Axel Heiberg Island and throughout the Arctic: General northward tendencies. *Polish Polar Research* 32 (3), 199-238. doi: 10.2478/v10183−011−0015−7

Evans, I.S., 2012 Geomorphometry and landform mapping: what is a landform? *Geomorphology,* 137 (1), 94-106. In 'Geospatial Technologies and Geomorphological Mapping', Proceedings of the 41st Annual Binghamton Geomorphology Symposium. [On-line 23 March 2011.]

Minár J., **Evans I.S.** & Krcho J., 2013 Geomorphometry: Quantitative Land-Surface Analysis. In: John F. Shroder (ed.) *Treatise on Geomorphology*, Volume 14, pp. 22-34. San Diego: Academic Press. (Section 2 of vol.14, D. Kennedy & A. D. Switzer (Eds.) Methods in Geomorphology | Investigating form.)

Stokes, Chris R., Shahgedanova, Maria, **Evans, Ian S.** & Popovnin, Victor, 2013 Response of small continental glaciers to recent climate change: Kodar Mountains, south-eastern Siberia. *Global & Planetary Change* 101, 82-96.

Evans, I. S. 2013 Major Scale Forms. In: Elias S.A. (ed.) *The Encyclopedia of Quaternary Science*, Vol. 1, pp. 847-864. Amsterdam: Elsevier. [Evans, D.J.A. (sub- ed.) Glacial landforms] [Second Edition]

Brown, Victoria H., Evans, David J.A., Vieli, Andreas & **Evans, Ian S.** 2013 The Younger Dryas in the English Lake District: reconciling geomorphological evidence with numerical model outputs. *Boreas* 42 (4), 1022-1042. *10.1111/bor.12020. ISSN 0300-9483.*

Minár, J., Jenčo, M., Pacina, J., **Evans, I. S.,** Minár, J. Jnr., Krcho, J., Kadlec, M., Burián L., Benová, A. 2013 Third-order geomorphometric variables (derivatives) – definition, computation and utilization of changes of curvatures. *International J of GIS.* 27 (7), 1381-1402. *http://dx.doi.org/10.1080/13658816.2013.792113*

Drăguţ , Lucian, Csillik, Ovidiu, Minár, Jozef, & **Evans Ian S.** 2013 Land-surface segmentation to delineate elementary forms from Digital Elevation Models. *Proceedings of Geomorphometry 2013:* Nanjing Conference, 42-45. [Extended abstract] *http://geomorphometyry.org/Dragut2013*

Evans Ian S. 2013 Land surface derivatives. *Proceedings of Geomorphometry 2013:* Nanjing Conference, 5-8. [Extended abstract] *http://geomorphometry.org/Evans2013* *http://geomorphometry.org/content/geomorphometry-2013-programme*

Mîndrescu, M. & **Evans, I.S.** 2014 Cirque Form and Development in Romania**:** Allometry and the buzz-saw hypothesis. *Geomorphology* 208, 117–136.

Csillik, O., **Evans, I. S.,** Drăguţ, L. 2015 Transformation (normalization) of slope gradient and surface curvatures, automated for statistical analyses from DEMs. *Geomorphology* 01/2015; 232. DOI:10.1016/j.geomorph.2014.12.038

Evans, I.S. 2015 The Lake District cirque inventory: updated. In McDougall DA and Evans DJA (eds.) *The Quaternary of the Lake District: Field Guide.* Quaternary Research Association, London, 65-82 [+ References consolidated at end of book]. ISSN: 0261 3611.

Evans, I.S., Hall, A.M., Kleman, J. 2015 Glacial cirques and the relationship between equilibrium line altitudes and mountain range height: COMMENT. *Geology* 43; e366. doi: 10.1130/G36667C.1

Csillik, O., **Evans, I. S.,** Drăguţ, L. 2015 Automated transformation of slope and surface curvatures to avoid long tails in frequency distributions. In: Jasiewicz J., Zwoliński Zb., Mitasova H., Hengl T. (eds), *Geomorphometry for Geosciences.* Adam Mickiewicz University in Poznań - Institute of Geoecology and Geoinformation, International Society for Geomorphometry, Poznań, *Geomorphometry2015*. geomorphometry.org, 119-122. [Extended abstract] *http://geomorphometry.org/Csillik2015*

Evans I.S., Cox N.J. 2015. Size and shape of glacial cirques: comparative data in specific geomorphometry. In: Jasiewicz J., Zwoliński Zb., Mitasova H., Hengl T. (eds), *Geomorphometry for Geosciences.* Adam Mickiewicz University in Poznań - Institute of Geoecology and Geoinformation, International Society for Geomorphometry, Poznań, *Geomorphometry2015*. geomorphometry.org, 79-82. [Extended abstract] *http://geomorphometry.org/EvansCox2015*

Minár, Jozef, Minár Jozef Jr & **Evans Ian S.** 2015 Towards exactness in geomorphometry. In: Jasiewicz J., Zwoliński Zb., Mitasova H., Hengl T. (eds), *Geomorphometry for Geosciences.* Adam Mickiewicz University in Poznań - Institute of Geoecology and Geoinformation, International Society for Geomorphometry, Poznań, *Geomorphometry2015*. geomorphometry.org, 27-30. [Extended abstract] *http://geomorphometry.org/Minar2015*

Gomez, C., Oguchi, T. & **Evans I.S.** 2015 Spatial Analysis in Geomorphology (1): Present Directions, from Collection to Processing (Editorial). In: C. Gomez, T. Oguchi and I.S. Evans (Eds.) Geomorphology in the Geocomputing Landscape: GIS, DEMs, Spatial Analysis and statistics *Geomorphology* 242, 1-2. doi:10.1016/j.geomorph.2015.04.026

Gomez, C., Oguchi, T., & **Evans, I.S.** 2016 Quantitative Geomorphology with Geographical Information Systems (GIS) for Evolving Societies and Science (Editorial). In: C. Gomez, T. Oguchi and I.S. Evans (Eds.) Geospatial Sciences - Acquisition and Processing for 21st Century Geomorphological Challenges. *Geomorphology*, 260, 1-3. doi: 10.1016/j.geomorph.2016.01.019

Evans, Ian S. 2016 Thoughts of a Semi-Retired Physical and Quantitative Geographer. *The Arab World Geographer / Le Géographe du monde arabe* Vol 19, no. 1-2, 56-62.

Minár J., **Evans I.S.** & Krcho J., 2016. Geomorphometry: Quantitative Land-Surface Analysis (2nd. Edition). In: *Reference Module in Earth Systems and Environmental Sciences*. Elsevier, Amsterdam.

Mîndrescu, Marcel & **Evans, Ian S.** 2016 Glacial cirques in the Romanian Carpathians and their climatic implications. Ch.9 in: Rădoane, M. and Vespremeanu-Stroe, A. *(eds.), Landform Dynamics and Evolution in Romania.* Springer International Publishing Switzerland 2017 DOI 10.1007/978-3-319-32589-7_9

Barr, Iestyn D., Ely, Jeremy C., Spagnolo, Matteo, Clark, Chris D., **Evans**, **Ian S.,** Pellicer, Xavier M., Pellitero, Ramón, Rea, Brice R. 2017 Climate patterns during former periods of mountain glaciation in Britain and Ireland: Inferences from the cirque record. *Palaeogeography, Palaeoclimatology, Palaeoecology* 485, 466-475.

Evans, Ian S. & Cox, Nicholas J. 2017 Comparability of cirque size and shape measures between regions and between researchers. *Zeitschrift für Geomorphologie* 61, Suppl. 2, 81-103. *Special Issue*.

Evans, Ian S. 2017 The glacial buzzsaw and its limitations: Mountain glaciation in British Columbia and in Britain. EXTENDED ABSTRACT. In: Niculiță, Mihai and Mărgărint, Mihai Ciprian (eds.), Proceedings of the Romanian Geomorphology Symposium 33rd edition, Iaşi, 11-14 May 2017. Editura Universității "Alexandru Ioan Cuza" din Iași. SNG2017_ISSN_2559-3021_47

Jozef Minár, Peter Bandura, Juraj Holec, Anton Popov, Michal Gallay, Jaroslav Hofierka, Ján Kaňuk, **Ian S. Evans** 2018 Physically-based land surface segmentation: Theoretical background and outline of interpretations. EXTENDED ABSTRACT, 4pp. *Geomorphometry 2018* Geomorphometry.org

Niculiţă Mihai, **Evans, Ian S.** 2018 Effects of glaciation on the clinometry and hypsometry of the Romanian Carpathians. EXTENDED ABSTRACT, 4pp. *Geomorphometry 2018* Geomorphometry.org

Allan M. Findlay, **Ian S. Evans** 2018 Population geography, scale, environment, and sex-ratio imbalances: An appreciation of the contribution to population geography of Professor John Clarke (1929-2018). *Population, Space and Place* (Sept.)

Ian S. Evans, Allan M. Findlay 2018 John Innes Clarke OBE, 7 January 1929 - 3 May 2018 *Geographical Journal* (Dec)

Le Chai, Wei Zhang, **Ian S Evans**; Liang Liu; Yapeng Li; Jingru Qiao; Qianyu Tang; Bo Sun. 2018 Geomorphic Features of Quaternary Glaciation in the Middle Section of the Tayantaweng Range, on the southeastern Qinghai-Tibet Plateau. *Journal of Mountain Science* (Chinese Academy of Sciences)